Ecological Monographs, 73(2), 2003, pp. 301–330

ESTIMATING COMMUNITY STABILITY AND ECOLOGICAL INTERACTIONS FROM TIME-SERIES DATA

A. R. Ives,[1,4,5] B. Dennis,[2,4] K. L. Cottingham,[3,4] and S. R. Carpenter[1,4]

[1]*Department of Zoology, University of Wisconsin, Madison, Wisconsin 53706 USA*
[2]*Department of Fish and Wildlife Resources and Division of Statistics, University of Idaho, Moscow, Idaho 83844-1136 USA*
[3]*Department of Biology, Dartmouth College, Hanover, New Hampshire 03755 USA*
[4]*National Center for Ecological Analysis and Synthesis, University of California, Santa Barbara, California 93101-5504 USA*

Abstract. Natural ecological communities are continuously buffeted by a varying environment, often making it difficult to measure the stability of communities using concepts requiring the existence of an equilibrium point. Instead of an equilibrium point, the equilibrial state of communities subject to environmental stochasticity is a stationary distribution, which is characterized by means, variances, and other statistical moments. Here, we derive three properties of stochastic multispecies communities that measure different characteristics associated with community stability. These properties can be estimated from multispecies time-series data using first-order multivariate autoregressive (MAR(1)) models. We demonstrate how to estimate the parameters of MAR(1) models and obtain confidence intervals for both parameters and the measures of stability. We also address the problem of estimation when there is observation (measurement) error. To illustrate these methods, we compare the stability of the planktonic communities in three lakes in which nutrient loading and planktivorous fish abundance were experimentally manipulated. MAR(1) models and the statistical methods we present can be used to identify dynamically important interactions between species and to test hypotheses about stability and other dynamical properties of naturally varying ecological communities. Thus, they can be used to integrate theoretical and empirical studies of community dynamics.

Key words: community matrix; community stability; multivariate autoregressive process; reactivity; resilience; stationary distribution; stochastic population model; time-series analysis; vector autoregressive process.

Introduction

The stability of ecological communities depends on at least three components of community structure: diversity (species richness), species composition, and the pattern of interactions among species. Much of the current scientific discussion of community stability focuses on diversity, because the relationship between diversity and community stability is central to arguments for preserving ecological diversity (Ehrlich and Daily 1993, Schulze and Mooney 1993, Tilman and Downing 1994, Schläpfer and Schmid 1999). However, the role of diversity in community stability is intimately linked to species composition and the pattern of interactions among species (Vitousek 1990, Walker 1992, Lawton and Brown 1993, Vitousek and Hooper 1993, Tilman 1996, Hooper and Vitousek 1997, Tilman et al. 1997, Ives et al. 1999*b*, 2000*b*). Composition is important because the presence of particular species within a community could change how the community responds to particular environmental perturbations (McNaughton 1977, 1985, Frank and McNaughton 1991). For example, a zooplankton species that is particularly tolerant to low pH could make the total zooplankton biomass in a community more stable against acidification (Frost et al. 1995). The pattern of interactions among species is important because the responses of individual species to environmental perturbations depend not only on the direct effect of the perturbation on their reproduction and mortality rates, but also on the indirect effects acting through changes in the abundances of other species in the community (May 1974, Holt 1977, Paine 1980, Pimm 1984, Abrams 1987, Carpenter et al. 1994*b*, Ives 1995*b*, McCann et al. 1998, Klug et al. 2000). Thus, understanding community stability requires understanding the combined effects of diversity, composition, and the patterns of interactions among species.

Community stability may be measured in many different ways. Most common measures of stability require systems to have an equilibrium point, or at least a well defined ''normal'' state from which deviations can be measured. Resilience (sensu Pimm 1984) is measured by the characteristic rate at which the abundances of populations within a community return to equilibrium following a disturbance. Resistance is a

Manuscript received 26 June 2001; revised 25 February 2002; accepted 26 February 2002; final version received 12 April 2002. Corresponding Editor: N. J. Gotelli.
[5] E-mail: arives@wisc.edu

measure of the magnitude of displacement of population abundances from equilibrium when subjected to a disturbance. Both of these concepts of stability can be modified for cases in which there is no strict equilibrium point (Steinman et al. 1992, Cottingham and Schindler 2000). Nonetheless, they are still based on the responses of systems away from their normal states. It is difficult to apply these measures to systems that are continuously buffeted by environmental fluctuations such that the normal state includes frequent disturbances.

An alternative approach is to view the dynamics of a community as a stochastic process and to define stability in terms of properties of a stochastic model of populations within the community. Such a stochastic model describes how the means, variances, and other statistical moments of population densities change through time. The equilibrium of a stochastic model is the joint stationary distribution of population abundances, and analogues of the deterministic concepts of the return time, resilience, and resistance can be defined with reference to this stationary distribution. As we will describe below, community stability may be measured by several different properties of the stochastic model. All of these properties share the advantage of being readily estimated directly from data. This is important, because disentangling the effects of diversity, species composition, and species interactions on community stability requires robust statistical techniques to analyze data from different ecological communities.

Our goals here are twofold. First, we describe different properties of stochastic processes that can be used to define stability. We focus on a particular type of stochastic process: first-order multivariate (or vector) autoregressive processes, abbreviated MAR(1) (Judge et al. 1985, Reinsel 1997). In MAR(1) processes, the changes in population abundances from time point $t - 1$ to the next time t depend only on the population abundances at time $t - 1$ and environmental disturbances occurring between time $t - 1$ and t; population abundances and environmental disturbances before time $t - 1$ have no direct effect. The first-order process implies that enough information can be obtained about a community at a single point in time to predict the immediate changes in species' abundances. In addition, MAR(1) processes assume that the interactions among species, and between species and environmental variables, are linear (at least after variables have been suitably transformed). MAR(1) models provide relatively simple approximations to nonlinear, non-first-order processes and therefore can be used to describe the general stochastic properties of complex communities (Ives 1995*a*, *b*).

Our second goal is to provide the statistical tools to estimate the strengths of interactions between species and the stochastic properties of the dynamics of communities from time-series data. For a community with a given number of species, the dynamics depend on how each species is affected by environmental fluctuations, measured in terms of changes in the species' population growth rates. The dynamics also depend on how changes in the abundance of species caused by environmental fluctuations in turn cause changes in the population growth rates of other species via species-species interactions. Interactions between species can be viewed as a filter that amplifies, either weakly or strongly, the variability in species' population growth rates caused by environmental fluctuations (Ives et al. 2000*b*). Thus, estimating the stability properties of a community necessarily requires estimating the strength of interactions between species. We approach this second goal by first describing statistical procedures for parameter estimation and model selection. We then illustrate these procedures by applying them to an example data set taken from a whole-lake experiment designed to assess the response of planktonic communities to environmental disturbances.

Road map

Developing both the theoretical measures of stability and the statistical methods to apply these measures to data is a formidable task, and some readers may want to skim some sections of this article. Therefore, we will begin with a road map. The destination is an analysis of seven years of data taken at weekly intervals over the summer from three experimentally manipulated lakes. The data set contains many of the features and puzzles found in other ecological data sets. Presenting a brief overview of the data here will help to motivate the theoretical and statistical development in the first parts of the article.

The data consist of weekly samples of zooplankton and phytoplankton, which for the analyses were divided into two zooplankton groups (*Daphnia* and non-*Daphnia*) and two phytoplankton groups (large and small phytoplankton). *Daphnia* are large, effective herbivores, and small phytoplankton are particularly vulnerable to herbivory, so we anticipated strong interactions between *Daphnia* and small phytoplankton groups. The experimental manipulations involved reconfiguring the initial fish composition of one lake so that the fish community was dominated by planktivorous fish that reduced *Daphnia* abundance, while the other two lakes were dominated by piscivorous fish that reduced the abundance of planktivorous fish, and hence had high *Daphnia* abundance. Then, over the course of seven years, nutrients were added to two of the lakes, the lake dominated by planktivores and one of the lakes dominated by piscivores.

The objective of the experiment was to ask how differences in the fish food webs among lakes altered the response of the planktonic community to nutrient addition (Carpenter et al. 2001). Here, however, we focus on a different question: How stable are the planktonic communities in the different lakes? Not surprisingly, the two lakes subjected to nutrient addition showed

greater variability over the seven years of the experiment as they responded to this perturbation. But we are specifically interested in the question: If these direct responses to the nutrient perturbations were factored out, thereby creating a theoretical level playing field for comparison, which lake would be the most stable? We are not interested in the stability of the lakes in the face of the nutrient perturbation per se, but instead are interested in the processes that affect the variability of the planktonic communities independently of this specific perturbation. When subjected to continuous environmental perturbations from all sources, which lake is most stable, and how do differences in the interactions within and among planktonic groups in the different lakes dictate differences in stability?

We address these questions by fitting a MAR(1) model to the data, and extracting different measures of stability from the fitted model. In the article, we begin by describing the relevant theoretical properties of MAR(1) processes (section *First-order autoregressive models*). Although MAR(1) models are linear (at least in transformed variables), we show how they can be derived as approximations to nonlinear systems. We then describe three different types of measures of stability (section *Stability properties of MAR(1) models*). The first is based on the variability of the stationary distribution of the stochastic process, whereas the second is based on the rate at which the stochastic process converges to the stationary distribution. The third, reactivity, is a measure of how strongly population abundances are pulled towards the mean of the stationary distribution. Much of the mathematical development of this section is relegated to the Appendix.

We then present statistical methods for fitting MAR(1) models to data. To begin, we show how to extend the standard MAR(1) model to account for some of the complexities likely to be encountered when addressing ecological data (section *Model modifications*). We show how measured environmental factors, such as nutrient addition in the lake data set, can be factored into MAR(1) models. We also consider observation error, the error unavoidable in ecological data that results from our inability to measure the ''true'' state of a system and the environmental variables that affect it. Methods for parameter estimation are then presented, including techniques to calculate approximate confidence intervals for not only the parameters of the MAR(1) model, but also aggregate parameters, specifically, our measures of stability (section *Model selection and statistical inference*). After presenting the needed statistical methods, we apply them to the lake data set (section *Limnological example*).

Much of this work is mathematically nontrivial, and we have not shied away from giving formal mathematical results that are needed to implement and modify our analyses. To make the concepts more approachable, however, we end each section with a descriptive summary of the major results from the section. Also, while we present formal results, we generally do not give proofs, but instead give references where similar results are derived. Finally, the programs used in our analyses of the lake data are available in ESA's Electronic Archive (Supplement).

First-Order Autoregressive Models

Below, we review some basic concepts of first-order autoregressive processes. We begin with the univariate case for a single species, and then develop the multivariate case. We also relate the autoregressive models to their deterministic counterparts; this makes it possible to show the correspondence between concepts of stability in stochastic models to the more familiar concepts applied in the stability analysis of deterministic models.

Univariate AR(1) process

A deterministic model frequently used to describe density-dependent population growth is a discrete-time Gompertz model (Reddingius 1971, Dennis and Taper 1994)

$$n_t = n_{t-1}\exp[a + (b - 1)\ln n_{t-1}]. \quad (1)$$

Here, n_t is population abundance, a is the intrinsic rate of increase, and b governs the strength of density dependence, with no density dependence corresponding to $b = 1$. As b decreases, density dependence increases, and when $b < 0$ overcompensating density dependence occurs in which population trajectories tend to show ''boom–bust'' patterns, with high and low densities alternating between successive time points. On a log scale, the model is a simple linear difference equation

$$x_t = a + bx_{t-1} \quad (2)$$

where $x_t = \ln n_t$. The Gompertz equation is only one of many simple models that have been applied to ecological systems (e.g., Zeng et al. 1998). We start with the Gompertz equation, because it is a log-linear model that often gives a reasonable first-order approximation to other nonlinear models.

Provided $b \neq 1$, this model has an equilibrium point x_∞ given by

$$x_\infty = a/(1 - b). \quad (3)$$

The condition for the equilibrium to be stable can be seen from the solution of the model given by Eq. 2. Starting from the initial point x_0 and substituting for a in terms of x_∞, it is easy to derive through recursion that

$$x_t = x_\infty + b^t(x_0 - x_\infty). \quad (4)$$

Thus, provided $|b| < 1$, x_t will converge to x_∞, with convergence occurring more quickly the closer $|b|$ is to zero. If $0 < b < 1$, convergence will occur monotonically, while damped two-point oscillations will occur when $-1 < b < 0$.

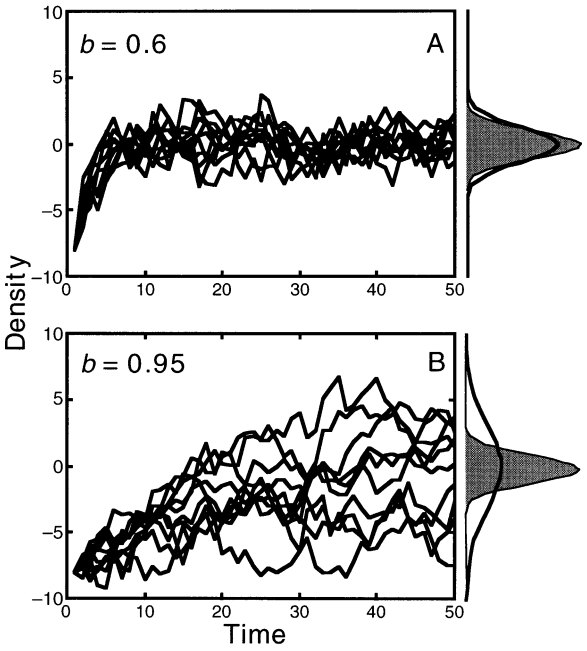

FIG. 1. Examples of two univariate AR(1) processes (Eq. 5) with autoregression parameter (A) $b = 0.6$ and (B) $b = 0.95$; $a = 0$ in both panels. Each panel shows 10 trajectories starting from the point $x_0 = -8$. The distribution of process errors E_t is normal with mean 0 and $\sigma^2 = 1$, which is depicted as the shaded area at the right in both panels. The stationary distribution is also normal and is shown as the heavy line to the right of the panels.

A stochastic version of Eq. 2 is the univariate AR(1) process

$$X_t = a + bX_{t-1} + E_t. \tag{5}$$

Here, X_t is log abundance at time t (in upper case to denote a random process), and E_t is a normal random variable with mean 0 and variance σ^2, and with $E_1, E_2, \ldots$ all independent. The random variable E_t represents "process error" or fluctuations caused by unspecified stochastic forces. In ecological terms E_t represents environmentally driven fluctuations in the per capita population growth rate and thus gives the environmental variability experienced by the population (see Dennis et al. 1991, Dennis and Taper 1994). The univariate AR(1) process has been an important model in the theory and statistical testing of density dependence (Dennis and Taper 1994 give a review). Properties of AR(1) processes can be found in texts that emphasize the statistical theory of time series (Harvey 1993, Box et al. 1994).

Fig. 1 gives two examples of univariate autoregressive processes for $b = 0.6$ and $b = 0.95$. Each panel displays 10 separate realizations of the same process. We will refer to this figure below to illustrate properties of autoregressive processes.

Univariate stationary distribution

The equilibrium for the AR(1) process X_t is the stationary distribution, which is the probability distribution approached by the distribution of X_t as $t \to \infty$ provided $|b| < 1$. Note that $|b| < 1$ is the same criterion for stability as for the corresponding deterministic model given in Eq. 2. The stationary distribution for X_t is a normal distribution with mean μ_∞ and variance υ_∞ given by (Box et al. 1994)

$$\mu_\infty = a/(1 - b) \tag{6}$$

$$\upsilon_\infty = \sigma^2/(1 - b^2). \tag{7}$$

The mean of the stationary distribution is the same as the deterministic point equilibrium (Eq. 3). The variance υ_∞ around the mean is directly proportional to the environmental variability, σ^2. It also depends on b, with values of b closer to zero corresponding to less population variability. Note that this coincides with values of b that produce rapid returns to equilibrium in the corresponding deterministic model (Eq. 4). In Fig. 1, the stationary distributions are given at the right margin of each panel (heavy line) along with the distribution of the process error E_t (shaded).

Univariate transition distribution

The transition distribution is the conditional probability distribution for X_t at any time t given that at time zero the initial condition is known to be $X_0 = x_0$. The transition distribution is normal, and both the mean and the variance depend on time t:

$$\mu_t = \mu_\infty + b^t(x_0 - \mu_\infty) \tag{8}$$

$$\upsilon_t = \sigma^2[1 + b^2 + (b^2)^2 + \cdots + (b^2)^{t-1}] = \sigma^2\left[\frac{1 - (b^2)^t}{1 - b^2}\right] = \upsilon_\infty[1 - (b^2)^t]. \tag{9}$$

Here $\mu_t = \mathrm{E}[X_t | X_0 = x_0]$ denotes the expected value of X_t, and $\upsilon_t = \mathrm{E}[(X_t - \mu_t)^2 | X_0 = x_0]$ denotes the variance of X_t given the initial condition $X_0 = x_0$. The formula for μ_t is identical to the solution trajectory for x_t in the deterministic model (Eq. 4). Note that if $|b| < 1$, then μ_t converges to μ_∞ and υ_t converges to υ_∞ as t becomes large. For small values of t, the transition distribution starts as a spike of probability near the initial size x_0 and then broadens to the stationary distribution as t becomes large. Thus, in Fig. 1 all trajectories begin at the same point, but then depart from each other as the transition distribution approaches the stationary distribution.

Multivariate AR(1) process

If there are p interacting species, a multivariate version of the univariate AR(1) model (Eq. 5) is

$$\mathbf{X}_t = \mathbf{A} + \mathbf{B}\mathbf{X}_{t-1} + \mathbf{E}_t \tag{10}$$

where $\mathbf{X}_t$ is a $p \times 1$ vector of (log-transformed) population abundances at time t, $\mathbf{A}$ is a $p \times 1$ vector of constants, $\mathbf{B}$ is a $p \times p$ matrix whose elements b_{ij} give the effect of the abundance of species j on the per capita population growth rate of species i, and $\mathbf{E}_t$ is a $p \times 1$

vector of process errors that has a multivariate normal distribution with mean vector $\mathbf{0}$ and covariance matrix $\mathbf{\Sigma}$. The vectors $\mathbf{E}_t$ represent stochastic environmental factors and are assumed to be independent through time. Nonetheless, the elements in $\mathbf{E}_t$ may covary with each other, as measured by the off-diagonal elements of the covariance matrix $\mathbf{\Sigma}$. Thus, if a good time interval for species i is also likely to be good for species j, then the element σ_{ij} in $\mathbf{\Sigma}$ will be positive.

MAR(1) models as approximations to nonlinear systems

The MAR(1) model can be viewed as a linear approximation to a nonlinear first-order stochastic process. Specifically, consider the model

$$\mathbf{X}_t = \mathbf{f}(\mathbf{X}_{t-1}, \mathbf{R}_t) \tag{11}$$

where $\mathbf{R}_t$ is a $q \times 1$ normal random variable with mean $\mathbf{0}$ representing the effects of q environmental variables on the population growth rate of the species, and $\mathbf{f}$ is a nonlinear function. If the stochastic process defined by Eq. 11 has a stationary distribution with mean $\mathbf{X}_\infty$, the right-hand side of Eq. 11 can be approximated using a first-order Taylor expansion around $\mathbf{X} = \mathbf{X}_\infty$ and $\mathbf{R} = \mathbf{0}$ to give

$$\mathbf{X}_t \approx \mathbf{f}(\mathbf{X}_\infty, \mathbf{0}) + \frac{\partial \mathbf{f}}{\partial \mathbf{X}}(\mathbf{X}_\infty, \mathbf{0})[\mathbf{X}_{t-1} - \mathbf{X}_\infty] + \frac{\partial \mathbf{f}}{\partial \mathbf{R}}(\mathbf{X}_\infty, \mathbf{0})\mathbf{R}_t \tag{12}$$

where $(\partial \mathbf{f}/\partial \mathbf{X})(\mathbf{X}_\infty, \mathbf{0})$ and $(\partial \mathbf{f}/\partial \mathbf{R})(\mathbf{X}_\infty, \mathbf{0})$ denote the partial derivatives of $\mathbf{f}$ with respect to the vectors $\mathbf{X}_{t-1}$ and $\mathbf{R}_t$, respectively, evaluated at $\mathbf{X}_t = \mathbf{X}_\infty$ and $\mathbf{R}_t = \mathbf{0}$. Thus, $(\partial \mathbf{f}/\partial \mathbf{X})(\mathbf{X}_\infty, \mathbf{0})$ is a $p \times p$ matrix with the i–jth element given by $\delta f_i/\delta X_j$, and $(\partial \mathbf{f}/\partial \mathbf{R})(\mathbf{X}_\infty, \mathbf{0})$ is a $p \times q$ matrix with the i–jth element given by $\delta f_i/\delta R_j$. This approximation is identical in form to the MAR(1) model given in Eq. 10, as can be seen by letting $\mathbf{B} = (\partial \mathbf{f}/\partial \mathbf{X})(\mathbf{X}_\infty, \mathbf{0})$, $\mathbf{A} = \mathbf{f}(\mathbf{X}_\infty, \mathbf{0}) - \mathbf{B}\mathbf{X}_\infty$, and $\mathbf{E}_t = (\partial \mathbf{f}/\partial \mathbf{R})(\mathbf{X}_\infty, \mathbf{0})\mathbf{R}_t$. Note that this explicitly defines the elements of $\mathbf{B}$ in terms of the interaction strengths between species; b_{ij} equals $\delta f_i/\delta X_j$, the change in the log population growth rate of species i with respect to changes in the log population abundance of species j. This approximation is contingent on the stochastic process being stationary. This is not an important restriction to our discussion, however, because all of the concepts of stability that we address apply to stationary processes.

In addition to being a linear approximation to nonlinear stochastic processes, Eq. 10 gives the stochastic equivalent of the deterministic multispecies Gompertz model. More generally, the matrix $\mathbf{B}$ contains the same information as the ''community matrix'' calculated to determine the stability properties around equilibrium of nonlinear deterministic models (May 1974, Pimm 1982). To see this, consider the deterministic version of the nonlinear stochastic model in Eq. 11

$$\mathbf{n}_t = \mathbf{h}(\mathbf{n}_{t-1}) \tag{13}$$

where $\mathbf{n}_t$ is a $p \times 1$ vector of (untransformed) population densities, and $\mathbf{h}$ is a nonlinear function. The community matrix of Eq. 13 is $(\partial \mathbf{h}/\partial \mathbf{n})(\mathbf{n}_\infty)$, the partial derivative of $\mathbf{h}$ with respect to $\mathbf{n}$ evaluated at the deterministic equilibrium, $\mathbf{n}_\infty$. The elements of $(\partial \mathbf{h}/\partial \mathbf{n})(\mathbf{n}_\infty)$ have the form $\delta h_i/\delta n_j$. Letting $f_i = \ln h_i$ and $x_j = \ln n_j$,

$$\left.\frac{\partial f_i}{\partial x_j}\right|_{x_\infty} = \left.\frac{\partial(\ln h_i)}{\partial(\ln n_j)}\right|_{n_\infty} = \left.\frac{n_j}{h_i}\frac{\partial h_i}{\partial n_j}\right|_{n_\infty} = \left.\frac{n_j}{n_i}\frac{\partial h_i}{\partial n_j}\right|_{n_\infty} \tag{14}$$

with the last step using the equality $h_i(\mathbf{n}_\infty) = n_i$ at equilibrium. Thus, the matrix $\mathbf{B} = (\partial \mathbf{f}/\partial \mathbf{X})(\mathbf{X}_\infty, \mathbf{0})$ differs from the community matrix $(\partial \mathbf{h}/\partial \mathbf{n})(\mathbf{n}_\infty)$ in having every row i multiplied by n_i and every column j multiplied by $(1/n_j)$. It is straightforward to show that matrix $\mathbf{B}$ and the community matrix have identical eigenvalues. Since the eigenvalues of the community matrix determine the population dynamics around equilibrium, matrix $\mathbf{B}$ contains the same information as the community matrix about population dynamics.

In summary, the MAR(1) model given by Eq. 10 is a linear approximation to more general nonlinear first-order autoregressive processes. The matrix of species interactions $\mathbf{B}$ is similar to the community matrix used to calculate the stability properties of nonlinear deterministic models. It is not surprising, therefore, that useful stability properties of the MAR(1) model can be defined in terms of properties of the matrix $\mathbf{B}$, as we show next.

MAR(1) stationary distribution

The MAR(1) process $\mathbf{X}_t$ has a stationary distribution provided all eigenvalues of matrix $\mathbf{B}$ lie within the unit circle (Harvey 1989, Reinsel 1997). This is identical to the criterion for stability of the point equilibrium in the corresponding deterministic model (May 1974). When the process error of the MAR(1) process is normally distributed, the stationary distribution is a multivariate normal distribution with mean vector $\boldsymbol{\mu}_\infty$ and covariance matrix $\mathbf{V}_\infty$ given by

$$\boldsymbol{\mu}_\infty = (\mathbf{I} - \mathbf{B})^{-1}\mathbf{A} \tag{15}$$

$$\mathbf{V}_\infty = \mathbf{B}\mathbf{V}_\infty\mathbf{B}' + \mathbf{\Sigma} \tag{16}$$

where $\mathbf{I}$ is the $p \times p$ identity matrix, and $\mathbf{B}'$ denotes the transpose of $\mathbf{B}$. Eq. 16 is a matrix equation that cannot be symbolically solved for the covariance matrix $\mathbf{V}_\infty$. However, one can use the ''Vec'' operator on both sides of Eq. 16 to obtain an explicit equation for the elements of $\mathbf{V}_\infty$. The operation Vec($\mathbf{A}$) creates a column vector out of any matrix $\mathbf{A}$ by stacking columns of $\mathbf{A}$ on top of each other, with the first column on the top and the last column on the bottom. The often-handy algebra of the Vec operator is reviewed by Searle (1982), and Judge et al. (1985:949–950) provide some basic identities. The resulting explicit equation for the elements of $\mathbf{V}_\infty$ is

$$\text{Vec}(\mathbf{V}_\infty) = (\mathbf{I} - \mathbf{B} \otimes \mathbf{B})^{-1}\text{Vec}(\mathbf{\Sigma}). \quad (17)$$

The symbol $\otimes$ denotes the Kronecker or direct matrix product; $\mathbf{M} \otimes \mathbf{N}$ is formed by scalar multiplying $\mathbf{N}$ in turn by each element of $\mathbf{M}$ and arranging the results into a large matrix. Thus, in Eq. 17 $\mathbf{B} \otimes \mathbf{B}$ is the $p^2 \times p^2$ matrix given by

$$\mathbf{B} \otimes \mathbf{B} = \begin{bmatrix} b_{11}\mathbf{B} & b_{12}\mathbf{B} & \cdots & b_{1p}\mathbf{B} \\ b_{21}\mathbf{B} & b_{22}\mathbf{B} & \cdots & b_{2p}\mathbf{B} \\ \vdots & \vdots & & \vdots \\ b_{p1}\mathbf{B} & b_{p2}\mathbf{B} & \cdots & b_{pp}\mathbf{B} \end{bmatrix}. \quad (18)$$

Eq. 17 is the multivariate analog to the univariate stationary variance equation (Eq. 7).

MAR(1) transition distribution

The transition distribution of $\mathbf{X}_t$ conditional on the initial value of $\mathbf{X} = \mathbf{x}_0$ is a multivariate normal distribution with mean vector $\boldsymbol{\mu}_t$ and covariance matrix $\mathbf{V}_t$ that change with time:

$$\boldsymbol{\mu}_t = \boldsymbol{\mu}_\infty + \mathbf{B}^t(\mathbf{x}_0 - \boldsymbol{\mu}_\infty) \quad (19)$$

$$\mathbf{V}_t = \mathbf{\Sigma} + \mathbf{B}\mathbf{\Sigma}\mathbf{B}' + (\mathbf{B}^2)\mathbf{\Sigma}(\mathbf{B}^2)' + \cdots + (\mathbf{B}^{t-1})\mathbf{\Sigma}(\mathbf{B}^{t-1})'. \quad (20)$$

Eq. 20 can be vectorized to obtain

$$\begin{aligned}\text{Vec}(\mathbf{V}_t) &= [\mathbf{I} + \mathbf{B} \otimes \mathbf{B} + (\mathbf{B} \otimes \mathbf{B})^2 + \cdots \\ &\quad + (\mathbf{B} \otimes \mathbf{B})^{t-1}]\text{Vec}(\mathbf{\Sigma}) \\ &= [\mathbf{I} - (\mathbf{B} \otimes \mathbf{B})^t][\mathbf{I} - \mathbf{B} \otimes \mathbf{B}]^{-1}\text{Vec}(\mathbf{\Sigma}). \quad (21)\end{aligned}$$

Eqs. 19 and 21 reduce to the univariate counterparts Eqs. 8 and 9. It is straightforward to show that the eigenvalues of the Kronecker product $\mathbf{B} \otimes \mathbf{B}$ are equal to the products of all the pairs of eigenvalues of $\mathbf{B}$: $\lambda_i\lambda_j$, $i = 1, \ldots, p$, $j = 1, \ldots, p$ (Seber 1984). Thus, if all eigenvalues of $\mathbf{B}$ lie within the unit circle, then all of the eigenvalues of $\mathbf{B} \otimes \mathbf{B}$ also lie within the unit circle. Therefore, $\mathbf{B}^t \to 0$ and $(\mathbf{B} \otimes \mathbf{B})^t \to 0$, and consequently $\boldsymbol{\mu}_t \to \boldsymbol{\mu}_\infty$ and $\mathbf{V}_t \to \mathbf{V}_\infty$ as $t \to \infty$.

Stability Properties of MAR(1) Models

The stability of a MAR(1) model can be measured in numerous ways, each highlighting a different aspect of the dynamics. Here, we constrain the discussion to stationary processes (in which all the eigenvalues of $\mathbf{B}$ lie within the unit sphere), thus excluding the possibility of species extinction. Our question is therefore how stable is the system, rather than whether the system is stable or unstable. All three of the types of measures of stability that we present in detail have close conceptual and mathematical relationships, and they all involve the interplay between short-term environmental fluctuations (vector $\mathbf{E}_t$ in Eq. 10) and interactions between species (matrix $\mathbf{B}$).

Our first measure of stability quantifies how the variance of the stationary distribution compares to the variance of the process error (environmental variability). The more stable the system, the lower the variance of the stationary distribution relative to the variance of the process error. The second measure of stability depends on the rate at which the transition distribution approaches the stationary distribution. This is comparable to stability measured by characteristic return rates in deterministic systems (May 1974); rapid approach to the stationary distribution (i.e., the stochastic equilibrium) corresponds to a more stable system. Our final measure addresses the reactivity of the system, defined as the immediate response of a system following a perturbation (Neubert and Caswell 1997). A highly reactive system may frequently move further away from the mean of the stationary distribution, even though on average the system remains stable. The more reactive a system, the less stable it is. The mathematical details of these measures of stability are given in the Appendix, and here we just give heuristic descriptions.

Variance of the stationary distribution

Stability measured in terms of the relationship between the variance of the stationary distribution and environmental variability can be illustrated using the ball-in-basin diagram frequently used to illustrate stability in deterministic systems. In Fig. 2A, the balls in both the steep and shallow basins are subjected to continuous perturbations that occur randomly in either direction. Following each perturbation, the ball in the steep basin rolls rapidly towards the bottom of the basin, while the ball in the shallow basin rolls to the bottom slowly. As a result, the ball in the shallow basin spends more time away from the basin bottom, leading to a stationary distribution with greater variance than the ball in the steep basin.

For the multispecies case, the covariance matrix of the stationary distribution $\mathbf{V}_\infty$ depends on the covariance matrix of the process error $\mathbf{\Sigma}$ and the interactions between species encapsulated in the matrix $\mathbf{B}$. As a measure of stability, it is natural to use the variance of the stationary distribution relative to the variance of the process error (environmental variability). By standardizing by the variance of the process error, differences between the variances of the stationary distributions of different communities can be attributed to species interactions. In a relatively stable system, species interactions will cause the variance of the stationary distribution to be only slightly greater than the variance of the process error. In contrast, in a less stable system, species interactions will greatly amplify the environmental variance, thereby creating large variance in the stationary distribution relative to the variance of the process error.

Fig. 3A and B give an example of two systems containing two competitors having different stability properties. Both systems experience the same environmental variance; the distribution of process errors is depicted by the shaded circle giving the 95% probability

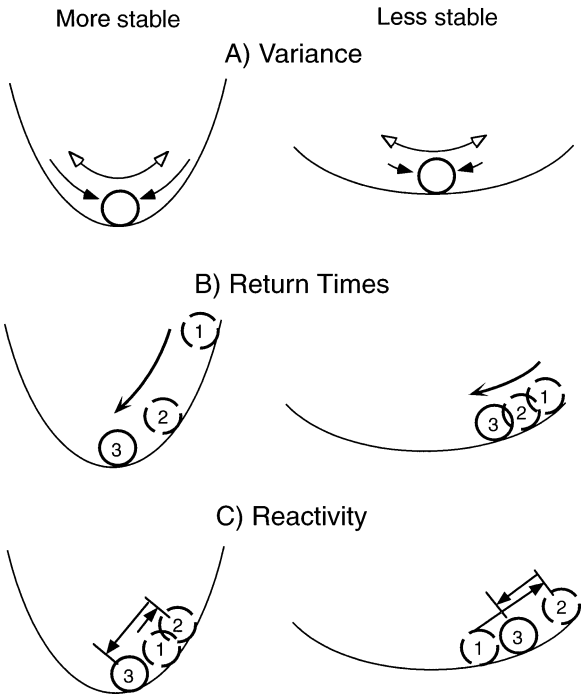

FIG. 2. Illustrations of three measures of stability. (A) The pair of balls-in-basins portray stability measured by the variance in the stationary distribution of the location of the ball. If subjected to the same disturbance regime (white arrows), the ball in the shallow basin on the right will spend more time away from the center of the basin, because the force to return to the center (solid arrows) is lower. This creates a stationary distribution with a greater variance. (B) The pair of balls-in-basins portrays stability measured by the return rate of the mean of the transition distribution to the mean of the stationary distribution. In the shallow basin, the ball will move more slowly to the center of the basin after being disturbed to the basin rim at location 1. (C) The pair of balls-in-basins portrays stability measured by the reactivity. In the steep basin, each successive location (1, 2, and 3) tends to bring the ball closer to the center of the basin than is the case for the shallow basin.

bounds of the distribution. In Fig. 3A, intra- and interspecific competition are relatively strong, leading to low variance in the stationary distribution compared to the system in Fig. 3B. Thus, the system in Fig. 3A is the more stable.

Although in this example it is easy to see the differences between systems, comparing the variances of stationary distributions for general, multidimensional systems is less straightforward. We use two methods, whose details are developed in the Appendix. The first involves measuring the variance in the stationary distribution along axes given by the eigenvectors of **B** (Ives 1995*a*). These eigenvectors are depicted by the axes in Fig. 3A and B. The variance in the stationary distribution along an eigenvector corresponding to a real eigenvalue, denoted $\tilde{v}_\infty$, is

$$\tilde{v}_\infty = \psi^2/(1 - \lambda^2) \qquad (22)$$

where ψ^2 is the variance of the process error along the eigenvector, and λ is the corresponding real eigenvalue. From this expression (as with b in Eq. 7 for a univariate AR(1) process), the closer the value of λ is to zero, the lower the variance of the stationary distribution along the corresponding eigenvector.

A similar result can be obtained for any complex eigenvalues of **B**. Complex eigenvalues occur in conjugate pairs, $\alpha \pm \beta i$, and the corresponding pair of eigenvectors defines a plane in the multidimensional space containing the stationary distribution. The sum of variances within this plane is

$$\tilde{v}^r_\infty + \tilde{v}^c_\infty = (\psi^r + \psi^c)/(1 - \|\alpha \pm \beta i\|^2) \qquad (23)$$

where $\tilde{v}^r_\infty$ and $\tilde{v}^c_\infty$ are variances of the stationary distribution along the two eigenvectors, ψ^r and ψ^c are variances of the process error, and $\|\alpha \pm \beta i\|$ is the magnitude of the eigenvalues. Thus, in the plane defined by the eigenvectors corresponding to a pair of complex eigenvalues $\alpha \pm \beta i$, the closer the magnitude of $\alpha \pm \beta i$ is to zero, the lower the variance of the stationary distribution.

The second method for comparing the variance of probability distributions uses determinants to measure the "volume" of covariance matrices. For example, in two-dimensional space the area of the parallelogram defined by any two vectors equals the determinant of the matrix containing the two vectors as columns. Since the covariance matrices $\mathbf{V}_\infty$ and $\mathbf{\Sigma}$ give the variances of the stationary distribution and process errors, respectively, the volume of the difference $\mathbf{V}_\infty - \mathbf{\Sigma}$ measures the degree to which species interactions increase the variance of the stationary distribution relative to the variance of the process error. From Eq. 16

$$\det(\mathbf{V}_\infty - \mathbf{\Sigma}) = \det(\mathbf{V}_\infty)\det(\mathbf{B})^2. \qquad (24)$$

Therefore, the proportion of the volume of $\mathbf{V}_\infty$ attributable to species interactions is $\det(\mathbf{V}_\infty - \mathbf{\Sigma})/\det(\mathbf{V}_\infty) = \det(\mathbf{B})^2$. The determinant of a matrix equals the product of its eigenvalues, so $\det(\mathbf{B})^2 = (\lambda_1\lambda_2 \cdots \lambda_p)^2$ for a community with p species. Since the magnitudes of the eigenvalues are less than one, this implies that $\det(\mathbf{B})^2$ will decrease with increasing numbers of species in a system, even if the eigenvalues have comparable magnitudes. Therefore, to facilitate comparisons among systems with different numbers of species, we use $\det(\mathbf{B})^{2/p} = (\lambda_1\lambda_2 \cdots \lambda_p)^{2/p}$. This is simply the square of the geometric mean of the eigenvalues.

These two methods for comparing the variances of stationary distributions (Eqs. 22 and 23 vs. Eq. 24) are related, since Eqs. 22 and 23 contain eigenvalues of **B**, and Eq. 24 contains $\det(\mathbf{B})$, which is the product of all eigenvalues. The former method can be compared to the most common measure of stability for deterministic models, the characteristic return rate. The characteristic return rate of a deterministic system depends on the dominant eigenvalue (i.e., the eigenvalue with the largest magnitude) of the community matrix

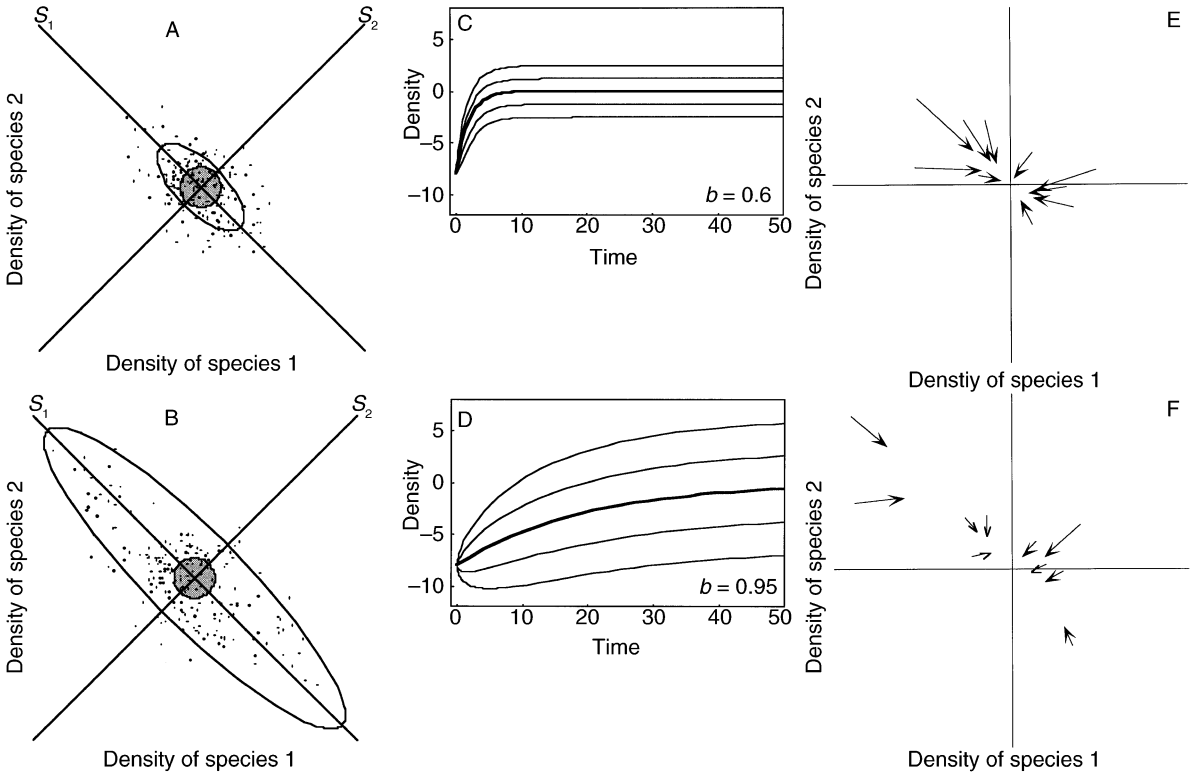

FIG. 3. Illustrations of measures of stability: (A, B), variance of the stationary distribution relative to the distribution of environmental process error; (C, D), characteristic return rates of the transition distribution to the stationary distribution; and (E, F), reactivity. For each pair of panels, the panel on the top gives the case of greatest stability. Panels A and B give the stationary distribution of a system made up of two competitors, with (A) $\mathbf{B}$ = [[0.6, −0.2], [−0.2, 0.6]] and (B) $\mathbf{B}$ = [[0.85,−0.1], [−0.1, 0.85]]; the MAR(1) process with these matrices was iterated 200 times to give the 200 points in the panels. The stationary distribution is given by the ellipse that incorporates 95% of the probability density of the stationary distribution. The shaded circle gives the 95% bounds of the process error, which is the same in panels (A) and (B). The lines give the eigenvectors corresponding to the eigenvalues (A) 0.8 and 0.4, and (B) 0.95 and 0.75. Panels (C) and (D) give the transition distributions for two univariate AR(1) processes for 50 time steps starting at $x_0 = -8$, with (C) $b = 0.6$ and (D) $b = 0.95$. The means of the transition distributions are given by the heavy lines, and the light lines give the mean ± 1 and 2 SD. Panels (E) and (F) give the case of two-competitor systems following MAR(1) processes with (E) $\mathbf{B}$ = [[0.3, −0.1], [−0.1, 0.3]] and (F) $\mathbf{B}$ = [[0.6, −0.2], [−0.2, 0.6]]. The arrows in each panel give the expected density (tip of the arrow) at time t for 10 points at time $t - 1$ (base of the arrow) selected from the stationary distribution.

(see the discussion after Eq. 14). Similarly, from Eqs. 22 and 23, the variance of the stationary distribution relative to the variance of the process error is greatest along the eigenvector corresponding to the dominant eigenvalue of $\mathbf{B}$, $\max(\lambda_{\mathbf{B}})$. Note, however, that a complete description of the variance of the stationary distribution depends on all of the eigenvalues of $\mathbf{B}$, not just the one with the greatest magnitude.

Rate of convergence of the transition distribution

When measuring the stability of deterministic models in terms of characteristic return rates, the equilibrium towards which the system returns is a point or (more rarely) some form of stable limit cycle. In stochastic models, the equilibrium is the stationary distribution. The rate of return to the stochastic equilibrium can be measured by the rate at which the transition distribution converges to the stationary distribution from an initial, known value of the system. The more rapid the convergence, the more stable the system. This is depicted for balls-in-basins in Fig. 2B, where the initial locations of the balls (labeled 1) are far from the bottom of the basin (the mean of the stationary distribution).

Different moments of the transition distribution may approach those of the stationary distribution at different rates. For simplicity, consider the univariate case. The rate at which the mean of the transition distribution approaches the mean of the stationary distribution is given by Eq. 8; if Δx_0 is the initial displacement of the mean of the transition distribution from the mean of the stationary distribution μ_∞, then the displacement at time t is $\Delta x_t = b^t \Delta x_0$. Thus, the characteristic rate at which Δx approaches 0 increases as $|b|$ gets smaller. In comparison, the variance of the transition distribution, υ_t, approaches the variance of the stationary distribution, υ_∞, more rapidly, with the characteristic rate of return scaling with b^2 (Eq. 9).

The rate of convergence of the transition distribution for a MAR(1) process is similar to the univariate process. The rate of return of the mean vector of $\mathbf{X}_t$ is governed by $\mathbf{B}$ (Eq. 19), and as in the deterministic case, the dominant eigenvalue of $\mathbf{B}$, $\max(\lambda_{\mathbf{B}})$, limits the return time of the mean to μ_∞. The rate of return of the covariance matrix, by contrast, involves the Kronecker product $\mathbf{B} \otimes \mathbf{B}$ (Eq. 21). The eigenvalues of the matrix $\mathbf{B} \otimes \mathbf{B}$ are the products of all the pairs of eigenvalues of $\mathbf{B}$: $\lambda_i\lambda_j$ ($i = 1, \ldots, p$; $j = 1, \ldots, p$). When the stationary distribution exists, the eigenvalue pair-products all have magnitudes smaller than $\max(\lambda_{\mathbf{B}})$. Thus, the elements of the covariance matrix of the transition distribution approach their equilibrium values rapidly compared to the elements in the mean vector. As in the case of the mean, the rate of return of the covariance matrix of the transition distribution to equilibrium is limited by the magnitude of the dominant eigenvalue of $\mathbf{B} \otimes \mathbf{B}$, $\|\max(\lambda_{\mathbf{B}\otimes\mathbf{B}})\|$, which equals $\|\max(\lambda_{\mathbf{B}})\|^2$.

The rate of convergence of the transition distribution to the stationary distribution is illustrated for a univariate system (Eq. 5) with $b = 0.6$ (Fig. 3C) and $b = 0.95$ (Fig. 3D) graphed as the mean $\pm$ 1 SD and $\pm$ 2 SD of the transition distribution; these give the same univariate processes as Fig. 1. In the univariate case, b is the single eigenvalue of the systems. In addition to showing that the mean of the transition distribution converges to that of the stationary distribution more rapidly when the magnitude of b is smaller, Fig. 3D also shows that the variance of the transition distribution approaches that of the stationary distribution more rapidly than the mean.

The rate of convergence of the transition distribution to the stationary distribution must be interpreted differently from the rate of convergence of the population size to equilibrium in deterministic models. In deterministic models, rapid return rates to equilibrium in a sense make a system more predictable. If there is some unknown perturbation at time $t = 0$, the population size will be close to equilibrium shortly thereafter if the rate of return to equilibrium is rapid. In stochastic models, the rate of convergence of the transition distribution to the stationary distribution is measured from some known observation $\mathbf{X}_0 = \mathbf{x}_0$. At time $t = 0$, we have full knowledge of the state of the system, because the variance of the transition distribution is zero. Through time, the variance of the transition distribution increases monotonically to that of the stationary distribution (Eqs. 9 and 19). Therefore, if the state of the system is known at a given point in time, information about the state of the system (i.e., the variance of $\mathbf{X}_t$ conditional on $\mathbf{X}_0 = \mathbf{x}_0$) is lost more rapidly if the variance of the stationary distribution returns to steady state more rapidly. This illustrates that, although there is a correspondence between the convergence rates to equilibrium in deterministic systems and the convergence rates of the mean of the transition distribution to the mean of the stationary distribution in stochastic systems, convergence rates of higher moments of stochastic processes do not have a counterpart in deterministic systems.

Reactivity

Neubert and Caswell (1997) warn that the commonly used concepts of stability involve long-term properties. For example, the rate of return of a deterministic system to equilibrium given by the dominant eigenvalue on the community matrix, $\max(\lambda_{\mathbf{B}})$, formally gives the asymptotic rate of return after short-term dynamics have dissipated following a perturbation. For management and other applications, properties of short-term system behavior might be of interest. Neubert and Caswell proposed various measures of transient system response to perturbations. One in particular is reactivity: a highly reactive system tends to move farther away from a stable equilibrium immediately after a perturbation, even though the system will eventually return to the equilibrium point. They proposed the concept of reactivity for continuous-time deterministic models, and here we develop the concept for stochastic models in discrete time.

Reactivity is illustrated in Fig. 2C. For a highly stable (unreactive) system, disturbances (depicted by the open arrows) may push a ball away from the bottom of the basin, yet on average the ball is pulled strongly towards the bottom of the basin between each successive time step. In contrast, in the shallow basin the same disturbances on a ball starting the same distance from the bottom of the basin may leave the ball farther from the bottom, because the ball is not brought strongly back towards the bottom between successive disturbances. This represents a more reactive system than that of the steep basin.

Fig. 3E and F give a numerical depiction of reactivity in the stochastic systems containing two competitors like in Fig. 3A and B. For each of 10 points, the arrows show the expected value of the system at the next time point. The system in Fig. 3E is unreactive, with the expected values of the system moving much closer to the mean of the stationary distribution between successive time steps. Conversely, in the more reactive system in Fig. 3F, the system moves only weakly toward the mean.

We use two methods to quantify the reactivity of a MAR(1) process. Both involve taking the mean of the expected change in distance from the mean of the stationary distribution between successive time steps, where this average is taken over the stationary distribution. Letting $\mathbf{X}_{t-1}$ denote the vector of population abundances at time $t - 1$, the squared Euclidean distance between $\mathbf{X}_{t-1}$ and the mean of the stationary distribution, μ_∞, is $\|\mathbf{X}_{t-1} - \mu_\infty\|^2 = (\mathbf{X}_{t-1} - \mu_\infty)'(\mathbf{X}_{t-1} - \mu_\infty)$. For a given value of $\mathbf{X}_{t-1}$, the expected value of $\mathbf{X}_t$ is $\mathrm{E}_{\varepsilon_{t-1}}[\mathbf{X}_t | \mathbf{X}_{t-1}] = \mathrm{E}_{\varepsilon_{t-1}}[\mathbf{A} + \mathbf{B}\mathbf{X}_{t-1} + \varepsilon_{t-1}] = \mathbf{A} + \mathbf{B}\mathbf{X}_{t-1}$. In Fig. 3E and F, if the base of a given arrow is $\mathbf{X}_{t-1}$, the tip of the arrow is the expectation given by

$\mathbf{A} + \mathbf{B}\mathbf{X}_{t-1}$. The squared Euclidean distance of this expectation from the mean of the stationary distribution is $\|\mathbf{A} + \mathbf{B}\mathbf{X}_{t-1} - \mu_\infty\|^2 = \|\mathbf{B}(\mathbf{X}_{t-1} - \mu_\infty)\|^2$; here we have used the relationship that $\mathbf{A} = (\mathbf{I} - \mathbf{B})\mu_\infty$ (Eq. 15). Therefore, the change in the squared Euclidean distance to μ_∞ between $\mathbf{X}_{t-1}$ and the expected value of $\mathbf{X}_t$ is $\|\mathbf{B}(\mathbf{X}_{t-1} - \mu_\infty)\|^2 - \|\mathbf{X}_{t-1} - \mu_\infty\|^2$.

As the first method for quantifying the reactivity of a MAR(1) process, we use the expectation of this difference when $\mathbf{X}_{t-1}$ is distributed according to the stationary distribution, scaled by the expectation of $\|\mathbf{X}_{t-1} - \mu_\infty\|^2$. In the Appendix, we show that

$$\frac{\mathrm{E}_{\mathbf{X}_\infty}[\|\mathbf{B}(\mathbf{X}_{t-1} - \mu_\infty)\|^2] - \mathrm{E}_{\mathbf{X}_\infty}[\|\mathbf{X}_{t-1} - \mu_\infty\|^2]}{\mathrm{E}_{\mathbf{X}_\infty}[\|\mathbf{X}_{t-1} - \mu_\infty\|^2]} = -\frac{\mathrm{tr}[\mathbf{\Sigma}]}{\mathrm{tr}[\mathbf{V}_\infty]} \quad (25)$$

where $\mathrm{tr}[\mathbf{\Sigma}]$ and $\mathrm{tr}[\mathbf{V}_\infty]$ are the traces of $\mathbf{\Sigma}$ and $\mathbf{V}_\infty$. The trace of a covariance matrix is simply the sum of variances of the constituent random variables, so $\mathrm{tr}[\mathbf{V}_\infty]$ is the sum of variances of individual species abundances. If the variance of the stationary distribution measured by $\mathrm{tr}[\mathbf{V}_\infty]$ is large relative to environmental variance measured by $\mathrm{tr}[\mathbf{\Sigma}]$, then the reactivity is relatively high. In other words, high reactivity corresponds to the case in which species interactions greatly amplify the environmental variance to produce a stationary distribution with high variances in the abundance of individual species.

In order to calculate the reactivity as quantified by Eq. 25, it is necessary to calculate the covariance matrix of the stationary distribution (Eq. 17). Thus, unlike the previous measures of stability, this requires information not only about $\mathbf{B}$ but also about the covariance matrix of the process error, $\mathbf{\Sigma}$, which is involved in determining the stationary distribution. This restriction can be removed using a second method to quantify reactivity. This involves calculating the ''worst-case'' scenario for reactivity, i.e., the maximum value of the quantity on the left-hand side of Eq. 25. In the Appendix, we show

$$\frac{\mathrm{E}_{\mathbf{X}_\infty}[\|\mathbf{B}(\mathbf{X}_{t-1} - \mu_\infty)\|^2] - \mathrm{E}_{\mathbf{X}_\infty}[\|\mathbf{X}_{t-1} - \mu_\infty\|^2]}{\mathrm{E}_{\mathbf{X}_\infty}[\|\mathbf{X}_{t-1} - \mu_\infty\|^2]} \leq \max(\lambda_{\mathbf{B}'\mathbf{B}}) - 1 \quad (26)$$

where $\max(\lambda_{\mathbf{B}'\mathbf{B}})$ is the dominant eigenvalue of the matrix $\mathbf{B}'\mathbf{B}$, the transpose of $\mathbf{B}$ multiplied by $\mathbf{B}$. Thus, using $\max(\lambda_{\mathbf{B}'\mathbf{B}}) - 1$ gives a method to characterize the ''worst-case'' reactivity of a system that depends only on the matrix $\mathbf{B}$.

Summary of stability properties

We have defined three types of measures of stability of a MAR(1) process. All three depend on the species interactions given in the matrix $\mathbf{B}$. The first type asks how interactions among species determine the variance of the stationary distribution relative to the environmental variance. Interactions between species act as a filter to amplify the environmental variability given by the process error $\mathbf{E}_t$. When species interactions greatly amplify the environmental variability, the variance of the stationary distribution is much greater than the variance of the process error, and the system can be said to be less stable. We give two ways to quantify the degree to which species interactions amplify environmental variability. The amplification can be measured by the eigenvalues of $\mathbf{B}$, which quantify the amplification in the directions given by the corresponding eigenvectors (Eqs. 22 and 23). The amplification can also be summarized by the quantity $\det(\mathbf{B})^{2/p}$, which gives a measure of the overall volume of the stationary distribution relative to the volume of the distribution of process error (Eq. 24).

The second type of measure of stability addresses the rate at which the transition distribution converges to the stationary distribution from a known point. The rate of convergence of the mean of the transition distribution is limited by the dominant eigenvalue of $\mathbf{B}$, $\max(\lambda_\mathbf{B})$ (Eq. 19). Therefore, $\max(\lambda_\mathbf{B})$ serves the same role as the dominant eigenvalue of the community matrix in the stability analysis of deterministic models. The rate of convergence of the variance of the transition distribution depends on the eigenvalues of $\mathbf{B} \otimes \mathbf{B}$, the maximum of which equals $\|\max(\lambda_\mathbf{B})\|^2$ (Eq. 21). Since for a stationary process $\|\max(\lambda_\mathbf{B})\| > \|\max(\lambda_\mathbf{B})\|^2$, the rate of convergence of the variance is more rapid than the rate of convergence of the mean.

The third measure of stability addresses the short-term dynamics occurring from one time point to the next. Reactivity is a measure of the displacement of the expected value of $\mathbf{X}_t$ from the mean of the stationary distribution relative to the displacement of $\mathbf{X}_{t-1}$ at the preceding time point. Reactivity can be quantified as the expectation over the stationary distribution of this change in displacement (Eq. 25). Alternatively, reactivity can be quantified for the ''worse-case'' scenario, which gives an expression for reactivity depending only on the matrix of species interactions, $\mathbf{B}$ (Eq. 26). The greater the variance of the individual species abundances relative to the variance of the process error, the higher the reactivity of the system, and hence the lower the stability. Therefore, just like the first measure of stability, greater variability of the stationary distribution relative to the environmental variability indicates lower stability.

Model Modifications

The MAR(1) processes discussed above can be modified to encompass a wide range of ecological situations. In addition to the state variables (variates) of the system (log population abundances), we may also have information about covariates, such as temperature, nutrient inputs, or other environmental factors that affect the dynamics of the system. These covariates can be

included in the MAR(1) model, thereby making it possible to account for long-term environmental trends and to address questions concerning the response of the system to known external disturbances. It is also possible to constrain the MAR(1) based on prior biological information. For example, elements of the matrix **B** (giving species interactions) may be set to zero if it is known that species do not interact, or the sign of an element could be set to positive or negative if the type of interaction between species is known. As a further modification, the MAR(1) model can be constructed to incorporate observation error. Observation error refers to any variability between the true values of variates and covariates in the MAR(1) model and the values that are observed. The most obvious source of observation error is measurement error, but more generally observation error occurs whenever the true variates and covariates that interact in the MAR(1) process are not known precisely. For example, even if air temperature were known without error, the temperature experienced by terrestrial animals would vary with wind speed, background substrate, topography, etc., making air temperature an imprecise estimate of the animals' true thermal regime. Observation error is ubiquitous in ecological systems and adds some complexities to fitting MAR(1) models to data.

Covariates and constraints

The MAR(1) model in Eq. 10 can be modified to include covariates:

$$\mathbf{X}_t = \mathbf{A} + \mathbf{B}\mathbf{X}_{t-1} + \mathbf{C}\mathbf{U}_t + \mathbf{E}_t \tag{27}$$

where $\mathbf{U}_t$ is a $q \times 1$ vector containing the values of q covariates at time t, and $\mathbf{C}$ is a $p \times q$ matrix whose elements c_{ij} give the strength of effect of covariate j on species i. The covariates $\mathbf{U}_t$ can be any factors that affect the system and may be transformed based upon either biological information about how the factors affect species' per capita population growth rates or the statistical properties of the MAR(1) model (see *Model selection and statistical inference*). Furthermore, while covariates may often be abiotic factors such as temperature, biotic factors may also be used. For example, in a study of interactions among phytoplankton and zooplankton, fish predation on the zooplankton may vary with the (known) number of fish in a lake. Because the system of interest consists of the phytoplankton and zooplankton, fish predation can be treated as a covariate (e.g., Ives et al. 1999*a*); the model includes the effect of fish predation on zooplankton, but does not consider the reciprocal effect of zooplankton on fish.

The covariates $\mathbf{U}_t$ differ from the other sources of environmental variability contained within the process error, $\mathbf{E}_t$, not only by being measured, but also by their statistical properties. The process error $\mathbf{E}_t$ is assumed to be temporally uncorrelated; $\mathbf{E}_1, \mathbf{E}_2, \ldots$ are all independent. In contrast, the covariates $\mathbf{U}_t$ need not be temporally uncorrelated, and in fact generally will not be. Thus, $\mathbf{U}_t$ can incorporate the effects of relatively slow environmental changes. For example, for data sets in which many samples are taken over the course of a season, it is reasonable to include seasonality; this can be done, for example, by including a sinusoidal function of day-of-year, or by including day-of-year and (day-of-year)^2 as covariates to model seasonal factors as a quadratic function (Ives et al. 1999*a*). Known and measured periodic environmental drivers can similarly be included. In addition, $\mathbf{U}_t$ may include categorical variables to fit the MAR(1) to data sets collected simultaneously at different locations. For example, suppose the MAR(1) model is being fitted simultaneously to the communities in two different lakes, and the researcher wants to include the possibility of differences in mean densities between lakes that are not explained by differences in measured covariates. The appropriate model would include a categorical variable $\mathbf{U}_{j,t}$ equaling zero for one lake and one for the other. The regression coefficients $\mathbf{C}_j$ calculated for $\mathbf{U}_{j,t}$ give the differences between lakes in the constant terms of the autoregression equations for each variate. Specifically, the constant terms for the first lake are $\mathbf{A}$, while the constant terms for the second lake are $\mathbf{A} + \mathbf{C}_j$.

With the addition of multiple covariates, the number of parameters in the MAR(1) model can become large, particularly when the number of species is large. Therefore, it is often desirable to reduce the number of parameters in the model based upon biological information about the system. For example, in a study of phytoplankton and zooplankton, nutrient input should have no direct effect on zooplankton, and therefore the coefficients in **C** for the effects of nutrient input on zooplankton can be set to zero. Similarly, the sign of elements of **B** and **C** may be known a priori. Therefore, when fitting the MAR(1) model these sign constraints may be imposed by setting to zero any spurious parameter estimates that arise when fitting a parameter-rich model, or by other techniques for constrained estimation. There are no set rules about how to structure the MAR(1) model; ecological knowledge of the particular system under study is essential.

The measures of stability we developed (see section *Stability properties of MAR(1) models*) apply only to basic MAR(1) processes with no covariates (Eq. 10). Nonetheless, there is no ambiguity in applying them to the MAR(1) model with covariates (Eq. 27). Most of the stability measures depend only on the matrix **B**, so the estimates of this matrix from Eq. 27 can be used directly. One measure of reactivity, Eq. 25, depends on the covariance matrix of the stationary distribution, and the stationary distribution in Eq. 27 depends on the covariates. We can, however, estimate the stationary distribution that would occur if the covariates were held constant by using **B** and the covariance matrix of the process error, $\mathbf{\Sigma}$, estimated from the full model with covariates, Eq. 27, thereby enabling the calculation of reactivity. When any measure of stability is applied to

a model with covariates, the measures assess the dynamics of the corresponding MAR(1) model in which the effects of the covariates have been factored out.

Observation error

Observation error occurs whenever the true values of the variates and covariates of the MAR(1) process are not precisely known. Observation error can be formally introduced into the MAR(1) model by separating the true values of the variates $\mathbf{X}_t^*$ and covariates $\mathbf{U}_t^*$ from those which are observed, $\mathbf{X}_t$ and $\mathbf{U}_t$:

$$\begin{aligned}\mathbf{X}_t^* &= \mathbf{A} + \mathbf{B}\mathbf{X}_{t-1}^* + \mathbf{C}\mathbf{U}_t^* + \mathbf{E}_t^* \\ \mathbf{U}_t^* &= \Theta(\mathbf{U}_{t-1}^*, \mathbf{U}_{t-2}^*, \ldots, \xi_t, \xi_{t-1}, \ldots) \\ \mathbf{X}_t &= \mathbf{X}_t^* + \mathbf{G}_t \\ \mathbf{U}_t &= \mathbf{U}_t^* + \mathbf{H}_t \end{aligned} \quad (28)$$

where $\mathbf{E}_t^*$ is the true process error, and $\mathbf{G}_t$ and $\mathbf{H}_t$ are normal random variables with mean $\mathbf{0}$ and covariance matrices $\mathbf{\Sigma}_G$ and $\mathbf{\Sigma}_H$ giving the observation error. This model assumes that observation errors are normally distributed (on a log scale) and are not temporally correlated. Also, if observation error for different variables taken at the same time are independent, then $\mathbf{\Sigma}_G$ and $\mathbf{\Sigma}_H$ will be diagonal matrices. The effects of observation error in the covariates on parameter estimation depend on the temporal autocorrelation structure of the covariates. Therefore, we assume the covariates $\mathbf{U}_t^*$ are an autoregressive integrated moving average (ARIMA) process (Box et al. 1994) governed by the linear function Θ in which values of $\mathbf{U}_t^*$ may depend on values in previous samples and normal random variables ξ_t with mean $\mathbf{0}$ and covariance matrices $\mathbf{\Sigma}_\xi$. For generality, we leave the order of the ARIMA process $\mathbf{U}_t^*$ unspecified.

The statistical complexity of the MAR(1) model with observation error can be illustrated using the univariate case with a single covariate. Writing Eq. 28 in terms of the observed variables X_t and U_t,

$$X_t = a + bX_{t-1} + cU_t + (G_t - bG_{t-1} - cH_t + E_t^*). \quad (29)$$

This is no longer an AR(1) process, for two reasons. First, the total error terms $E_t = (G_t - bG_{t-1} - cH_t + E_t^*)$ are not temporally independent, since E_t and E_{t-1} both depend on G_{t-1}. Thus, the total error term E_t is a moving average process (Box et al. 1994). Second, the total error term depends on the parameters b and c. If, for example, the value of b were positive, then the term $G_t - bG_{t-1}$ would cause the total error to be a moving average process with negative autocorrelation. This illustration demonstrates that analysis of the MAR(1) model with observation error must explicitly account for the covariance structure of the error term that includes both observation and process error.

Observation error can be incorporated into data analyses in several ways (Fuller 1987, Carpenter et al. 1994*a*, Hilborn and Mangel 1997). First, if independent estimates of observation error (matrices $\mathbf{\Sigma}_G$ and $\mathbf{\Sigma}_H$) are available, these can be incorporated directly (although care must be taken to estimate $\mathbf{\Sigma}_G$ and $\mathbf{\Sigma}_H$ under the same transforms as the data). Second, if the variance of the observation error is known relative to the variance of the process error, then this ratio can be incorporated into the model. Third, the variance of the observation error can be estimated from the data at the same time as the parameters and process error are estimated. This uses information about the correlation structure of the observed errors (Eq. 28) to estimate the elements of $\mathbf{\Sigma}_G$ and $\mathbf{\Sigma}_H$. We recommend against this third approach, however, because time-series data from ecological systems are often not extensive enough for accurate estimates of observation variances. We feel it is better to use even a rough independent estimate of the observation variance (in either absolute terms or relative to the process error) and then perform a simulation sensitivity analysis of the effect of observation error on the conclusions.

Summary of model modifications

The basic MAR(1) model (Eq. 10) can be modified to include covariates $\mathbf{U}_t$ for environmental factors other than species abundances (Eq. 27). This makes it possible to estimate how the system responds to measured external driving variables. It is also possible to structure the MAR(1) model to disallow interactions (set parameters to zero) or constrain the sign of interactions. Finally, observation error can be included (Eq. 28), although this produces a process that is no longer MAR(1) in the observed variates and therefore must be analyzed accordingly. With these modifications, however, the measures of stability that we derived in the preceding section remain unchanged; stability, as measured by the way in which interactions among species determine the properties of the stochastic process, still depends on the matrix $\mathbf{B}$. Covariates and observation error will certainly affect the estimated model of the observed process. Nonetheless, the measures of stability can still be interpreted unambiguously in terms of the stochastic properties of the true (unobserved) system in the absence of variability in the external drivers (covariates).

Parameter Estimation

Parameters of the MAR(1) model can be estimated using conditional least squares (CLS), maximum likelihood (ML), or a Bayesian framework (Schnute 1994). The first two approaches are described for general ecological time-series models by Dennis et al. (1995), and here we present the specific procedures for the MAR(1) model. In some situations the estimates from CLS and ML are identical, and in most situations the estimates

are close. Observation error requires a more complicated treatment, which we present in brief.

Conditional least squares (CLS)

The CLS estimates of parameters in the MAR(1) model are those values that minimize the squared difference between the observed population abundances at time t and those predicted by the MAR(1) model, conditional on the population abundances at time $t - 1$. To make the calculations explicit, it is easiest to state the MAR(1) model in full matrix form. For a data set with $T + 1$ data points, let $\mathbf{X}$ be the $T \times p$ matrix whose column i contains all of the observed data for species i, excluding the last observation at time T; $\mathbf{X} = [\mathbf{X}_0, \mathbf{X}_1, \ldots, \mathbf{X}_{T-1}]'$. Similarly, let $\mathbf{Y}$ be the $T \times p$ matrix of observed data excluding the first observation; $\mathbf{Y} = [\mathbf{X}_1, \mathbf{X}_2, \ldots, \mathbf{X}_T]'$. Finally, let $\mathbf{U} = [\mathbf{U}_1, \mathbf{U}_2, \ldots, \mathbf{U}_T]'$ be the $T \times q$ matrix of observed covariates and $\mathbf{E} = [\mathbf{E}_1, \mathbf{E}_2, \ldots, \mathbf{E}_T]'$ be the $T \times p$ matrix of process error terms. Then the MAR(1) model of Eq. 27 has the form

$$\mathbf{Y} = \mathbf{1}\mathbf{A}' + \mathbf{X}\mathbf{B}' + \mathbf{U}\mathbf{C}' + \mathbf{E} \tag{30}$$

where $\mathbf{1}$ is the $T \times 1$ vectors of ones. The CLS estimates of the parameters minimize, for each species i, the squared difference between predicted and observed population abundances one time step in advance, $(\mathbf{Y}_i - \hat{\mathbf{Y}}_i)'(\mathbf{Y}_i - \hat{\mathbf{Y}}_i)$, where $\hat{\mathbf{Y}}_i = (\hat{a}_i + \mathbf{X}\hat{\mathbf{B}}_i' + \mathbf{U}\hat{\mathbf{C}}_i')$, and $\hat{\mathbf{Y}}_i$, $\hat{a}_i$, $\hat{\mathbf{B}}_i$, and $\hat{\mathbf{C}}_i$ are the ith rows of the corresponding matrices of estimated parameters. Letting $\mathbf{Z} = [\mathbf{1}, \mathbf{X}, \mathbf{U}]$ be the $T \times (1 + p + q)$ matrix with $\mathbf{1}$, $\mathbf{X}$, and $\mathbf{U}$ concatenated horizontally as columns, and $\hat{\mathbf{D}}_i = [\hat{a}_i, \hat{\mathbf{B}}_i, \hat{\mathbf{C}}_i]$ be the $1 \times (1 + p + q)$ vector containing the estimates of a_i, $\mathbf{B}_i$, and $\mathbf{C}_i$, the CLS estimates are given by the formula

$$\hat{\mathbf{D}}_i' = (\mathbf{Z}'\mathbf{Z})^{-1}\mathbf{Z}'\mathbf{Y}_i. \tag{31}$$

These estimates are exactly the least squares estimates obtained using standard regression by treating $\mathbf{X}_t$ as a dependent variable, and $\mathbf{X}_{t-1}$ and $\mathbf{U}_t$ as independent variables. Note, however, that although the CLS estimates are the same, inference about the estimates (e.g., confidence intervals) are not the same as those one would obtain from standard regression, because the data are time series (see *Model selection and statistical inference: Parameter confidence intervals*).

The CLS estimators are asymptotically unbiased; their expected values equal the true parameter values as the sample size T gets infinitely large (Judge et al. 1985, Tong 1990). For small sample sizes, however, there can be considerable bias in CLS estimators, and this bias depends on the initial value $\mathbf{X}_0$ of the time series and the system itself, with systems having slow convergence to the stationary distribution typically leading to greater bias (Fuller 1996). Unfortunately, there is no easy way to estimate this bias or to determine what are ''small'' sample sizes. Nonetheless, the presence of bias and a rough indication of its sign and magnitude can be obtained from bootstrapping (see *Model selection and statistical inference: Parameter confidence intervals*).

Maximum likelihood

For any set of parameter values, it is possible to calculate the likelihood of the observed data under a specific MAR(1) model. The maximum likelihood parameter estimates are those parameter values that produce the greatest likelihood of the observed data (e.g., Hilborn and Mangel 1997). Under the assumptions that the process error terms $\mathbf{E}_t$ have a multivariate normal distribution with mean vector $\mathbf{0}$ and covariance matrix $\mathbf{\Sigma}$, and are temporally independent, the ML estimates are those values which minimize the negative log-likelihood function given by

$$L = \frac{pT}{2}\ln 2\pi + \frac{T}{2}\ln|\mathbf{\Sigma}| + \frac{1}{2}[\mathbf{Y} - (\mathbf{A}' + \mathbf{X}\mathbf{B}' + \mathbf{U}\mathbf{C}')] \times \mathbf{\Sigma}^{-1}[\mathbf{Y} - (\mathbf{A}' + \mathbf{X}\mathbf{B}' + \mathbf{U}\mathbf{C}')]'. \tag{32}$$

Note that, unlike CLS estimation, the elements of $\mathbf{\Sigma}$ are treated as parameters and are estimated simultaneously with the other parameters. If there are no a priori constraints placed on the parameters (e.g., all elements of $\mathbf{B}$ are estimated), then by matrix differentiation of L it can be shown that the ML estimates are identical to the CLS estimates. However, when there are constraints, the ML and CLS estimates differ, although in our experience the differences are small. Like CLS estimators, ML estimators also may be considerably biased for small sample sizes.

Obtaining the ML estimates requires minimizing L, which has up to $p(p + q + 1)$ parameters in $\mathbf{A}$, $\mathbf{B}$, and $\mathbf{C}$, and an additional $p(p + 1)/2$ parameters in $\mathbf{\Sigma}$. The Nelder-Mead simplex algorithm is convenient for minimization (Press et al. 1992), and many mathematical and statistical software packages include Nelder-Mead simplex routines (e.g., Matlab, Mathworks 1996). Although the computations are relatively straightforward, for systems with many species the computational time is much greater than that required to calculate the CLS estimates. Thus, for computationally intensive analyses, CLS estimates have advantages over ML estimates, particularly since in practice the estimates seem to be very close in general.

Observation error

Observation error introduces the two problems that the total error is temporally correlated and depends on the parameters of the MAR(1) process (see *Model modifications: Observation error*). Observation error therefore requires explicit attention to the covariance structure of the total error between successive samples.

What are the consequences of not taking observation error into account when in fact it occurs? Consider the simple case of the univariate AR(1) model without covariates (Eq. 5):

$$X_t^* = a + bX_{t-1}^* + E_t^* \qquad X_t = X_t^* + G_t. \quad (33)$$

For large sample sizes, the expectation of the CLS estimate of b computed from the observed variate X_t is

$$\mathrm{E}[\hat{b}] = \frac{\sigma_{yx}}{\sigma_{xx}} = \frac{\sigma_{y^*x^*}}{\sigma_{x^*x^*} + \sigma_{gg}} = \frac{b\sigma_{x^*x^*}}{\sigma_{x^*x^*} + \sigma_{gg}} \quad (34)$$

where σ_{yx} is the covariance between the observed random variables X_t and X_{t-1}, $\sigma_{y^*x^*}$ is the covariance between the X_t^* and X_{t-1}^*, and σ_{xx}, $\sigma_{x^*x^*}$, and σ_{gg} are the variances of X_{t-1}, X_{t-1}^*, and G_t (cf., Fuller 1987:3). Thus, the CLS estimate of b is biased towards zero, as also occurs in simple linear regression (Fuller 1987). Since $b = 1$ gives the case of no density dependence (i.e., the population dynamics exhibit random-walk behavior), Eq. 34 implies that in the univariate case observation error falsely increases estimates of the strength of density dependence (Shenk et al. 1998). For the multivariate case with covariates, the situation is more complex, and observation error could either increase or decrease the naive CLS estimate of density dependence.

We will illustrate an observation-error model for a univariate AR(1) process with observation error in both the variate and a single covariate. The effects of observation error in covariates on the estimates of coefficients for both variates and covariates depend on the temporal autocorrelation of the covariates. Therefore, it is necessary to analyze the covariates to determine their temporal structure; this can be done with standard model identification procedures (e.g., Box et al. 1994:181–223). For our example, we assume we know that the covariate follows an AR(1) process. An AR(1) model with observation error in which a single covariate follows an AR(1) process is given by

$$\begin{aligned} X_t^* &= a + bX_{t-1}^* + cU_{t-1}^* + \varepsilon_t \\ U_t^* &= d + fU_{t-1}^* + \xi_t \\ X_t &= X_t^* + g_t \\ U_t &= U_t^* + h_t \end{aligned} \quad (35)$$

where X_t^* and U_t^* are unobserved, and X_t and U_t are observed values of variate and covariate, respectively; ε_t and ξ_t are process errors for the variate and covariate; g_t and h_t are observation errors for variate and covariate; and a, b, c, d, and f are regression coefficients. In addition to these coefficients, the parameters of the model include the variances of ε_t, ξ_t, g_t, and h_t, denoted σ_ε^2, σ_ξ^2, σ_g^2, and σ_h^2, respectively. Note that Eq. 35 gives a bivariate AR(1) process in which the covariate U_t^* is treated as a variate.

Eq. 35 is in state-space form, and therefore for a given data set the likelihood function can be computed using a set of recursion equations known as the Kalman filter (Harvey 1989). The Kalman filter is a numerical procedure in which successive estimates of the unobserved values X_t^* in a time series are calculated sequentially by first predicting X_t^* from X_{t-1}^* and U_{t-1}^* using the autoregressive model (Eq. 35), and then updating these estimates using the observed value X_t. This procedure also computes the likelihood function and therefore can be used in ML parameter estimation with numerical minimization. Because the methods are straightforward and presented excellently by Harvey (1989), we present only the results of a sample analysis of Eq. 35.

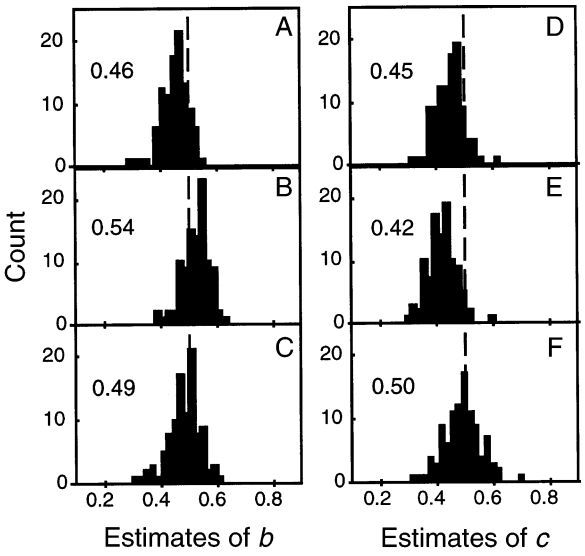

FIG. 4. Estimates of parameters b and c in an autoregressive model with observation error (Eq. 35) from (A, C) 100 simulated data sets using CLS estimation ignoring observation error, (B, E) a state–space model assuming observation error only in the variate, and (C, F) a state–space model assuming observation error in both variate and covariate. The true values are $b = c = 0.5$, and for the simulation the autoregression coefficient for the covariate was $f = 0.8$. Numbers in each panel give the mean of the estimates of the simulated data sets.

We generated 100 data sets from Eq. 35 for the case of a strongly autocorrelated covariate ($f = 0.8$). We then fit each data set using (1) CLS which ignores observation error in both X_t and U_t, (2) a state–space model in which observation error in U_t was ignored (i.e., setting $\sigma_h^2 = 0$ and treating Eq. 35 as a univariate AR(1) with covariates), and (3) the state-space model with observation error in both X_t and U_t given by Eq. 35. To fit the data, we assumed that the observation error variances, σ_g^2 and σ_h^2, were known, but then fit all other model parameters. Also, for the state–space models we assumed that the means and variances of the first observations of each data set equal the estimated means and variances of the stationary distribution.

Fig. 4 plots the 100 estimates of parameters b and c using each of the three methods. Ignoring observation error in both X_t and U_t (Fig. 4A, D) leads to underestimates of both parameters, while ignoring observation error in U_t but not X_t (Fig. 4B, E) overestimates b and underestimates c. These biases depend on the autocor-

relation of the covariate U_t; when this autocorrelation is zero ($f = 0$), the estimate of b is unbiased, although the estimate of c remains biased downwards (analyses not shown). Accounting for observation error in both variate and covariate, not surprisingly, gave less biased estimates (Fig. 4C, F), although the estimators are slightly more variable. Nonetheless, the ML estimates obtained from Eq. 35 are only asymptotically unbiased, and when applied to small samples (with ''small'' depending on the structure of the underlying process) the ML estimates can be noticeably biased (Fuller 1987: 164–173).

Summary of parameter estimation

Conditional least squares (CLS) estimation provides a computationally simple and fast way to fit a MAR(1) model to data (Eq. 31). The parameter estimates are those that would be obtained if standard regression were applied in which $\mathbf{X}_t$ were treated as dependent variables, and $\mathbf{X}_{t-1}$ and $\mathbf{U}_t$ were treated as independent variables. Maximum likelihood (ML) estimates (Eq. 32) are identical to CLS estimates for unstructured MAR(1) models (i.e., no constraints are placed on the parameters). Even when there are constraints, in our experience there is little difference between the CLS and ML estimates.

When there is observation error, estimates obtained from either CLS or ML will be biased. Therefore, accounting for observation error is important when determining the stability of a system, because bias in parameter estimates will also bias estimates of stability. For example, for simple univariate AR(1) processes, observation error biases the estimate of b towards zero (Eq. 34), thereby making the process appear more stable than it really is by any of the three measures of stability we propose. Estimation with observation error can be performed by modeling the process in state-space form and applying a Kalman filter to compute the likelihood function (e.g., Eq. 35). When there is observation error in the covariates, parameter estimates depend on the temporal autocorrelation structure of the covariates.

Model Selection and Statistical Inference

The preceding section has provided tools to estimate the parameters of a MAR(1) model, but how should the appropriate MAR(1) model be selected in the first place? Model selection has two components: specifying a particular MAR(1) and then performing diagnostics to determine whether the MAR(1) model adequately describes the data. Once a satisfactory model is identified, it can be used for statistical inference to obtain, for example, the confidence intervals for the model parameters. It is also possible to obtain confidence intervals for other estimable quantities, in particular the measures of stability we derived in the section *Stability properties of MAR(1) models*.

Model selection

The general form of the model, such as what variates and covariates to use, is dictated by the data in hand, the questions being addressed, and prior biological knowledge of the system. We can provide only the obvious rules of thumb that a useful statistical model is more likely if data sets are long, observation error is low, and the numbers of variates and covariates are small. Here, we deal with model selection once these broad decisions have been made. In particular, given a set of variates and covariates, what parameters of the MAR(1) model can be set to zero on statistical grounds, because their non-zero estimates do not improve the fit between the model and data?

Two criteria are commonly used in model selection, Akaike's Information Criterion (AIC) and the Bayesian Information Criterion (BIC):

$$\text{AIC} = 2L_{\min}/T + 2Q/T$$

$$\text{BIC} = 2L_{\min}/T + Q \log(T)/T \qquad (36)$$

where $L_{\min}$ is the value of the negative log-likelihood function calculated at the ML estimates, and Q is the total number of estimated parameters. The criteria are applied by selecting that model with the lowest AIC or BIC score. Both AIC and BIC incorporate a ''penalty factor'' for the number of parameters in a model ($2Q/T$ and $Q \log(T)/T$, respectively), thereby favoring a model that includes only those parameters which provide a minimum amount of additional information about the system (Box et al. 1994, Dennis et al. 1998). For BIC, the penalty factor is larger, so the BIC selects models with fewer parameters than the AIC.

The number of possible MAR(1) models from which to select can be large. There are various strategies for searching for the AIC or BIC selected model; we describe one strategy when we analyze our limnological example (see *Analysis of limnological data: model selection*). Any strategy will necessarily involve estimating parameters for many models, and obtaining ML estimates is prohibitively intensive computationally. Therefore, in searching for a lowest-AIC or lowest-BIC model, we suggest using the CLS parameter estimates rather than the ML estimates in calculating $L_{\min}$. The similarity between the CLS and ML estimates makes this a pragmatic approach. Computing ML estimates with observation error (e.g., Eq. 35) is much more intensive than ML estimation without observation error, so we restrict attention to model selection under the assumption of no observation error. Once a model is selected, the consequences of observation error for the parameter estimates can be determined.

Diagnostics

Once a MAR(1) model is selected, it should be examined to determine whether it gives a reasonable description of the data set. The diagnostics are based on the assumptions underlying the MAR(1), focusing on

the residuals between the observed log densities at t, $\mathbf{X}_t$, and those predicted from the MAR(1) model and the log densities $\mathbf{X}_{t-1}$ and covariates $\mathbf{U}_t$. Useful diagnostics are (Box et al. 1994, Fuller 1996):

1) Whether the residuals for each species are temporally autocorrelated, which can be determined using autocorrelation functions (ACF) and partial autocorrelation functions (PACF).

2) Whether the mean and/or variance of the residuals are correlated with any of the variates or covariates of the model, which is most easily determined by graphing the residuals or partial residuals (Neter et al. 1989:392) against the variates and covariates.

3) Whether the interactions among species or between species and covariates are nonlinear, which can be determined again by graphing the residuals against the variates and covariates and looking for curved relationships.

4) Whether the residuals are normally distributed, which can be determined from normal probability plots. In fact, the residuals need not be normally distributed to have a well-defined MAR(1) process, and CLS estimation does not assume that the error terms $\mathbf{E}_t$ are normal (Judge et al. 1985). Nonetheless, ML estimation and consequently AIC and BIC model selection do assume normality.

5) Whether the model explains much of the variance of the data. In ordinary (non-time-series) regression, it is usual to report the proportion of the total variance of the dependent variables explained by the model. In time-series analysis, values of $\mathbf{X}_{t-1}$ are used to predict $\mathbf{X}_t$. Therefore, it is most informative to ask what proportion of the change in log density from time $t - 1$ to time t is explained by the MAR(1) model (e.g., Ives et al. 1999*a*). This can be measured with the conditional R^2, which is the typical R^2 applied to the change in log densities. Often, a fitted model will explain more of the total variance in log density than the variance in the change in log density between consecutive samples, so the total R^2 will generally be greater than the conditional R^2.

These diagnostics are simply guides to determine whether the model fit is adequate and to suggest possible measures to take to produce a better model, such as transforming covariates. If the diagnostics show that the model fails, there are numerous tactics that can be tried to correct the model (Box et al. 1994).

Parameter confidence intervals

Once a well-fitting MAR(1) model has been found, the confidence intervals for its parameters can be calculated, thereby giving a statistical assessment of the values of coefficients contained in the model. Calculating confidence intervals must account for the covariance structure of time-series data. For example, even though the CLS parameter estimates are the same as those obtained from standard regression by treating $\mathbf{X}_t$ as a dependent variable and $\mathbf{X}_{t-1}$ as an independent variable, the variance of the CLS estimator for a time series is not the same as the variance of the corresponding standard regression estimator, and therefore the confidence intervals for the parameter estimates will be different (Dennis and Taper 1994).

To give a simple example of the consequences of the covariance structure of time-series data, consider the problem of calculating the mean of the stationary distribution, $\mu_\infty = a/(1 - b)$, of a univariate AR(1) process given by Eq. 5. The sample mean $\hat{\mu}_\infty = \bar{X} = (1/T)\,\Sigma_{t=1}^{T} X_t$ is an unbiased estimator of μ_∞, while its variance is

$$\begin{aligned}
\mathrm{V}[\hat{\mu}_\infty] &= \mathrm{V}\left[\frac{1}{T}\sum_{t=1}^{T} X_t\right] \\
&= \frac{1}{T^2}\mathrm{V}[(a + bX_0 + E_1) \\
&\qquad + (a + b(a + bX_0 + E_1) + E_2) + \cdots] \\
&= \frac{1}{T^2}\mathrm{V}\left[E_1\frac{1 - b^T}{1 - b} + E_2\frac{1 - b^{T-1}}{1 - b} + \cdots + E_T\right] \\
&= \frac{\sigma^2}{T^2}\frac{1}{(1 - b)^2}\left(T - 2\frac{1 - b^{T+1}}{1 - b} + \frac{1 - b^{2(T+1)}}{1 - b^2}\right) \\
&\approx \frac{\sigma^2}{T}\frac{1}{(1 - b)^2}. \qquad (37)
\end{aligned}$$

The factor σ^2/T is the variance of the estimator of the mean that would apply if the data were not temporally correlated, while $1/(1 - b)^2$ arises from the temporal autocorrelation of X_t. Obviously, when b is close to 1, the variance of the estimator of the mean becomes large. This is not surprising, because it will be difficult to estimate the mean of an AR(1) process that is close to a random walk, or in ecological terms, a population that experiences weak density dependence.

There are two approaches to obtain confidence intervals for parameters of MAR(1) models. The first uses bootstrapping (Efron and Tibshirani 1993, Dennis et al. 2001). This approach begins by obtaining parameter estimates; ML estimates can be used, although the computational speed of CLS estimation makes CLS more practical. Parameter estimation produces a $T \times p$ matrix of residuals $\mathbf{e}$, with each of the p columns corresponding to one of the p species in the system. Under the assumption of the MAR(1) model, the elements in each column should be uncorrelated and identically distributed. Therefore, they can be randomly sampled (with replacement) to create a new set of residuals, $\mathbf{e}_{\text{rand}}$. To maintain the covariance structure of errors for different species, the residuals $\mathbf{e}$ should be sampled as rows which contain the p residuals from the same time point (one for each species). Thus, $\mathbf{e}_{\text{rand}}$ is a $T \times p$ matrix whose rows are randomly sampled rows of the matrix $\mathbf{e}$. A bootstrapped data set is created by selecting an initial point, $\mathbf{x}_0$, calculating the predicted value for $\mathbf{x}_1$ using the MAR(1) model with

$\mathbf{X}_{t-1} = \mathbf{x}_0$ and $\mathbf{U}_t = \mathbf{u}_1$, adding the first element of $\mathbf{e}_{\text{rand}}$, and continuing in this manner for the remaining $T - 1$ points. The initial value $\mathbf{x}_0$ can be chosen as either the first observation in the real data set, or the predicted mean of the stationary distribution conditional on the observed values of the covariates $\mathbf{u}_0$; for long data sets, this choice makes little difference, while for short data sets we prefer the former approach if the real data set has relatively unstable dynamics (e.g., $\max(\lambda_{\mathbf{B}}) > 0.5$) and $\mathbf{x}_0$ is therefore likely to be far from the mean. The parameters are then estimated for the bootstrapped data set. Repeating this procedure with a new set of residuals $\mathbf{e}_{\text{rand}}$ for, say, 2000 bootstrapped data sets will produce 2000 bootstrapped estimates for each parameter. The $1 - \alpha$ confidence intervals are the intervals given by $\alpha/2$ and $(1 - \alpha/2)$ quantiles of the bootstrapped estimates. Joint confidence intervals can similarly be calculated from the joint distribution of bootstrapped parameter values. Finally, the bootstrapped data sets can be used to indicate whether the parameter estimators are biased (see *Parameter estimation*). Bias is indicated if the average parameter values from the bootstrapped data sets differ sizably and consistently from the estimates obtained from the data set from which the bootstrapped data sets are constructed. Methods for compensating for bias using bootstrapping are reviewed in Efron and Tibshirani (1993). Any approach, however, would have to be explored and justified for MAR(1) models using numerical simulation studies.

The rationale behind the bootstrapping approach is that, under the assumption that the fitted MAR(1) model is correct, the residuals form a consistent estimate of the process error distribution (Efron and Tibshirani 1993). Therefore, the confidence intervals represent the probability bounds for obtaining parameter estimates under the fitted MAR(1) process. Often one wants to know if a parameter differs from zero. In practice, if the confidence limits do not include zero, the parameter differs from zero. Departure from zero can be tested directly by structurally setting the parameter to zero, refitting the model, and using the refitted, reduced model to create bootstrapped data sets. The full and reduced model are fitted to each bootstrapped data set, and the likelihood ratio test statistic is calculated. The resulting bootstrapped test statistic values form a consistent estimator of the distribution of the test statistic under the null hypothesis that the parameter in question is zero. The likelihood ratio statistic for the actual data is compared to the desired percentile of the estimated null hypothesis distribution to conduct the hypothesis test (Dennis and Taper 1994). Note that this will test whether a parameter differs significantly from zero under the assumption that the values of all of the other parameters are those estimated from the MAR(1) model with the parameter in question set to zero. In other words, this test is conditional on the estimated values of other parameters.

A second approach to obtaining confidence intervals, called profile likelihood, takes advantage of the asymptotic chi-square distribution of a likelihood ratio test statistic. One constructs a likelihood ratio test of the null hypothesis that a parameter is equal to a known constant versus the alternative hypothesis that the parameter is not equal to that constant. The hypothesis test is inverted into a confidence interval; the set of all values of the constant for which the null hypothesis would not be rejected at level α is an approximate $100(1 - \alpha)\%$ confidence interval for the parameter. The technique requires that the null hypothesis model has a stationary distribution; otherwise, the likelihood ratio statistic does not have an approximate chi-square distribution. Dennis et al. (1995) demonstrate the profile likelihood technique for multivariate time-series population models. The technique can be adapted for CLS estimation using various chi-square statistics that arise under this type of estimation (Knight 2000).

Both of these approaches for obtaining confidence intervals assume that there is no observation error. When there is observation error in the covariates, parametric bootstrapping can be used. Parametric bootstrapping involves producing the bootstrap data sets by simulating the fitted model, rather than by resampling residuals. The data sets are created under the observation error MAR(1) model (Eq. 28), and the model is then refitted to each of the bootstrapped data sets. For large data sets with several variates, however, this is computationally prohibitive. Asymptotic confidence intervals for the observation error MAR(1) model can also be obtained from the log-likelihood function (cf., Judge et al. 1985), although this suffers from the requirement of large sample sizes.

Finally, we note that these procedures all assume that the model is known to be correct. In fact, the correct model is not known, and therefore the parameter confidence intervals are conditional on the model selected. As suggested by Zeng et al. (1998), it is conceivable to bootstrap over the collection of all possible models by creating bootstrapped data sets from the model including all admissible parameters, selecting the best-fitting model using AIC or BIC, and then estimating coefficients. However, the numerical intensity of this procedure makes it impractical with present-day computing power.

Confidence intervals for other quantities

Bootstrapping can be used not only to obtain confidence intervals for the parameter estimates, but also for any function of the parameters. Natural candidates of interest are the measures of stability in the section *Stability properties of MAR(1) models*. The procedure is the same as that outlined for bootstrapping parameter estimates; construct bootstrapped data sets using the best-fitting model, estimate the quantity in question from the bootstrapped data sets, and determine the con-

fidence intervals from the resulting distribution of bootstrap estimates.

Summary of model selection

Once the general form of a MAR(1) model is chosen (i.e., what variates and covariates to include), the best-fitting MAR(1) model can be selected based on a number of criteria; we suggest Akaike's Information Criterion (AIC) and the Bayesian Information Criterion (BIC). Model selection involves deciding which parameters to estimate and which to set to zero. Once the best-fitted model is selected, diagnostics should be performed to determine whether the fitted MAR(1) model adequately describes the data. Confidence intervals for the parameter estimates can be obtained either by bootstrapping or by profile likelihood. Finally, bootstrapping can also be used to obtain confidence intervals for any function of the parameters. This makes it possible to compare statistically the estimates of stability obtained from different ecological systems.

Limnological Example

To illustrate our measures of stability and the statistical methods for fitting a MAR(1) model, we use a data set of phytoplankton and zooplankton in three lakes. After describing the objectives of the experiment and the data set, we proceed by analyzing the data: selecting a MAR(1) model, obtaining parameter estimates, and estimating the stability of the different lake communities. We use this example to ask two questions about our approach. Do MAR(1) models yield parameter estimates that are sensible ecologically? And do the measures of stability inform us about differences in dynamics among lakes?

Objectives of the experiment

The roles of nutrients and predation in ecosystem dynamics are of great interest in both aquatic and terrestrial ecology (Pace et al. 1999, Persson 1999, Polis 1999). To examine the joint effects of nutrients and predation in lakes, Carpenter et al. (2001) added nutrients to two lakes with contrasting food webs, while a third unmanipulated reference lake was monitored. They found that nutrient enrichment caused a large increase in biomass of phytoplankton in Peter Lake, a system dominated by planktivorous fishes that selectively removed large-bodied *Daphnia*. In contrast, West Long Lake was dominated by piscivorous bass that reduced planktivorous fish and thereby increased *Daphnia* abundance. Heavy grazing by large *Daphnia* suppressed the response of phytoplankton to the nutrient enrichment in West Long Lake.

Description of the experiment and data set

The experiment is described in detail by Carpenter et al. (2001) and will be summarized briefly here. The food web of the reference lake, Paul Lake, was dominated by piscivorous largemouth bass throughout the experiment. West Long Lake's food web was dominated by piscivores (largemouth and smallmouth bass) and benthivorous yellow perch. Peter Lake was manipulated by removing bass in 1991 to reconfigure the food web to dominance by planktivorous minnow species. Beginning in 1993, Peter and West Long Lakes were enriched with nitrogen and phosphorus at a ratio chosen to be near the pre-manipulation ratio and maintain limitation by phosphorus. In this paper, we present data from two pre-enrichment years (1991 and 1992) and four years in which nutrients were added (1993–1996). We will refer to Paul, West Long, and Peter Lakes as the reference, the low planktivory, and the high planktivory lakes, respectively.

All three lakes were monitored weekly during the period of summer stratification (approximately mid May to early September each year). The samples started in midsummer in 1991, leading to nine samples in that year, while subsequent years yielded 17, 17, 17, 16, and 15 samples. The vast majority of summer samples were taken at 7-d intervals; of the total of 254 intervals between samples during the summer months, 242 (95%) were 7 d, whereas 3, 8, and 1 were 5, 6, and 8 d, respectively. Although the samples were not all taken at the same interval, because the vast majority were 7 d apart, we did not account for variation in time between samples in the analyses. Nutrient additions were measured directly. Here, we used additions of the most limiting nutrient (phosphorus) as a covariate. Natural inputs of phosphorus are small relative to the experimental inputs (Carpenter et al. 2001). We used potential planktivory on zooplankton as a second covariate. Potential planktivory was calculated as the biomass of fishes that could potentially consume zooplankton, based on species and body size. Only two fish samples were taken per year, at the beginning and end of summer stratification. We log-linearly interpolated between these points to obtain estimates of potential planktivory at the times of plankton samples.

We represented the planktonic food web by four functional groups. Phytoplankton biomass (as mg chlorophyll/m^2, integrated over the photic zone) was partitioned into small-particle (passing a 35-μm screen) and large-particle (retained by 35-μm screen) fractions. The small phytoplankton are readily consumed by all zooplankton grazers, while the large phytoplankton are generally susceptible only to *Daphnia*. Zooplankton biomass (as mg dry mass/m^2, integrated over the entire water column) was partitioned into *Daphnia* and non-*Daphnia* biomass, reflecting the important role of *Daphnia* as a grazer in these lakes. Methods for field sampling and laboratory analyzes are reported by Carpenter et al. (2001).

MAR(1) model selection

We fit the data from all lakes to the MAR(1) model of the form

$$\mathbf{X}_t = \mathbf{A} + \Delta\mathbf{A}_\mathbf{H} + \Delta\mathbf{A}_\mathbf{L} + (\mathbf{B} + \Delta\mathbf{B}_\mathbf{H} + \Delta\mathbf{B}_\mathbf{L})\mathbf{X}_{t-1} + \mathbf{C}\mathbf{U}_t + \mathbf{E}_t. \quad (38)$$

Matrix $\mathbf{B}$ contains coefficients for the interactions between variates (small phytoplankton, large phytoplankton, *Daphnia*, and non-*Daphnia*), matrix $\mathbf{C}$ gives the effects of environmental covariates (nutrient input and planktivorous fish biomass) on each species-group, and $\mathbf{A}$ is a vector of constants. Matrices denoted $\Delta\mathbf{B}_\mathbf{H}$ and $\Delta\mathbf{B}_\mathbf{L}$ represent differences between the $\mathbf{B}$ matrix for the reference lake and the $\mathbf{B}$ matrices for the high and low planktivory lakes, respectively; matrices $\Delta\mathbf{A}_\mathbf{H}$ and $\Delta\mathbf{A}_\mathbf{L}$ are defined similarly. To estimate the elements of matrices $\Delta\mathbf{B}$, we used the $T \times 4$ indicator matrices $\mathbf{\Phi}_\mathbf{H}$ and $\mathbf{\Phi}_\mathbf{L}$ whose elements for each sample equal one for the high and low planktivory lakes, respectively, and zero for the other two lakes. Thus, the model included variables $\mathbf{\Phi}_\mathbf{H}$ and $\mathbf{\Phi}_\mathbf{L}$ to obtain $\Delta\mathbf{A}_\mathbf{H}$ and $\Delta\mathbf{A}_\mathbf{L}$, and $\mathbf{\Phi}_\mathbf{H}\cdot\mathbf{X}_{t-1}$ and $\mathbf{\Phi}_\mathbf{L}\cdot\mathbf{X}_{t-1}$ to obtain $\Delta\mathbf{B}_\mathbf{H}$ and $\Delta\mathbf{B}_\mathbf{L}$, where $\cdot$ denotes the element-by-element product of the matrices (i.e., if $\mathbf{P} = \mathbf{M}\cdot\mathbf{N}$, then the i–jth element of $\mathbf{P}$ is $m_{ij}n_{ij}$).

Because data were only collected during the summer months, leading to a long unsampled interval between years, in the CLS and ML analyses we did not include transitions from the last sample in the fall and the first sample in the spring. The ways in which we treated between-year intervals for bootstrapping parameter confidence intervals and fitting observation-error models are discussed below (see *Parameter estimation and diagnostics*).

Analyzing the data simultaneously for all lakes has two advantages over fitting each lake separately. First, differences in the $\mathbf{B}$ matrices among lakes are captured explicitly in the matrices $\Delta\mathbf{B}_\mathbf{H}$ and $\Delta\mathbf{B}_\mathbf{L}$. Therefore, model fitting and statistical inference to identify differences among lakes involve determining whether the elements of $\Delta\mathbf{B}_\mathbf{H}$ and $\Delta\mathbf{B}_\mathbf{L}$ are non-zero. Second, the parameters of the model are estimated using data from all three lakes, thereby providing greater precision in estimation.

Rather than consider all possible models, we constrained the model on biological grounds. Specifically, we assumed that the planktivory manipulations had no direct effect on phytoplankton groups, and the nutrient addition had no direct effect on zooplankton groups. Further, we assumed that the *Daphnia* and non-*Daphnia* zooplankton groups did not have a direct effect on each other, but only interacted through their shared consumption of phytoplankton. Finally, we restricted some signs of interactions, excluding negative effects of phytoplankton on zooplankton and positive effects of phytoplankton on each other. To implement these sign restrictions, if the signs of interactions obtained in a fitted violated the restrictions, we forced the corresponding coefficient to be zero.

We selected the best model structure based on the AIC criterion in which parameters were estimated using CLS. To find the model with the lowest AIC, we randomly selected a model by including or excluding coefficients with equal probability. For each random initial model, we either added a coefficient that was initially excluded or subtracted a coefficient that was initially included. If the AIC of the resulting model decreased, we proceeded with the resulting model. Each coefficient in turn was tested, and then the procedure was looped so that coefficients were iteratively tested in sequence. This procedure continued until no improvements were made in the fit of the model. We repeated this procedure starting with 500 randomly constructed initial models. This procedure identified a best-fitting model and an additional four models with AIC values within 3 of the best-fitting model. Although the close values of AIC do not strongly support selecting the best-fitting model over the near alternatives, all models were similar, differing in only the presence/absence of single coefficients. Furthermore, the stability measures differed little among models; values of $\det(\mathbf{B})^{2/p}$ differed among all five models by 1.0%, 1.0%, and 3.0% for reference, high, and low planktivory lakes, respectively.

Parameter estimation and diagnostics

Fig. 5 shows the data from all three lakes, and Table 1 gives the CLS parameter estimates with 95% confidence intervals for the AIC best-fitting model. To obtain confidence intervals, we created bootstrapped data sets by starting variates at their observed values for each year of the data set, thereby making no assumptions about how densities at the end of one year affect densities at the beginning of the following year. Normal probability plots of the residuals (Fig. 6) demonstrate near normality, with the exception of a few points at the upper and lower tails of the distribution. The overall levels of planktivory (fish biomass) were very different among lakes, and using log-transformed planktivory reduced this difference. Therefore, we also performed the analyses using untransformed fish biomass, but the results were quantitatively very close to those obtained using log-transformed fish biomass, so we only report the results using log-transformed fish biomass. The PACFs of the residuals showed little evidence of autocorrelation (Fig. 7), although there was a high positive lag-4 partial autocorrelation of residuals of large phytoplankton; we have no biological explanation for this and believe it is not biologically significant.

The residuals obtained from CLS estimation were nearly normal. Therefore, it is not surprising that the ML estimates of model parameters are close to those obtained by CLS (Table 2). We calculated ML estimates only for the best-fitting model obtained using CLS due to the computational intensity of finding the best-fitting model using ML estimation. Thus, we assumed that ML and CLS estimates are similar enough to give the same best-fitting model.

We also estimated parameters with the observation-error model of Eq. 28 (Table 2), using independent

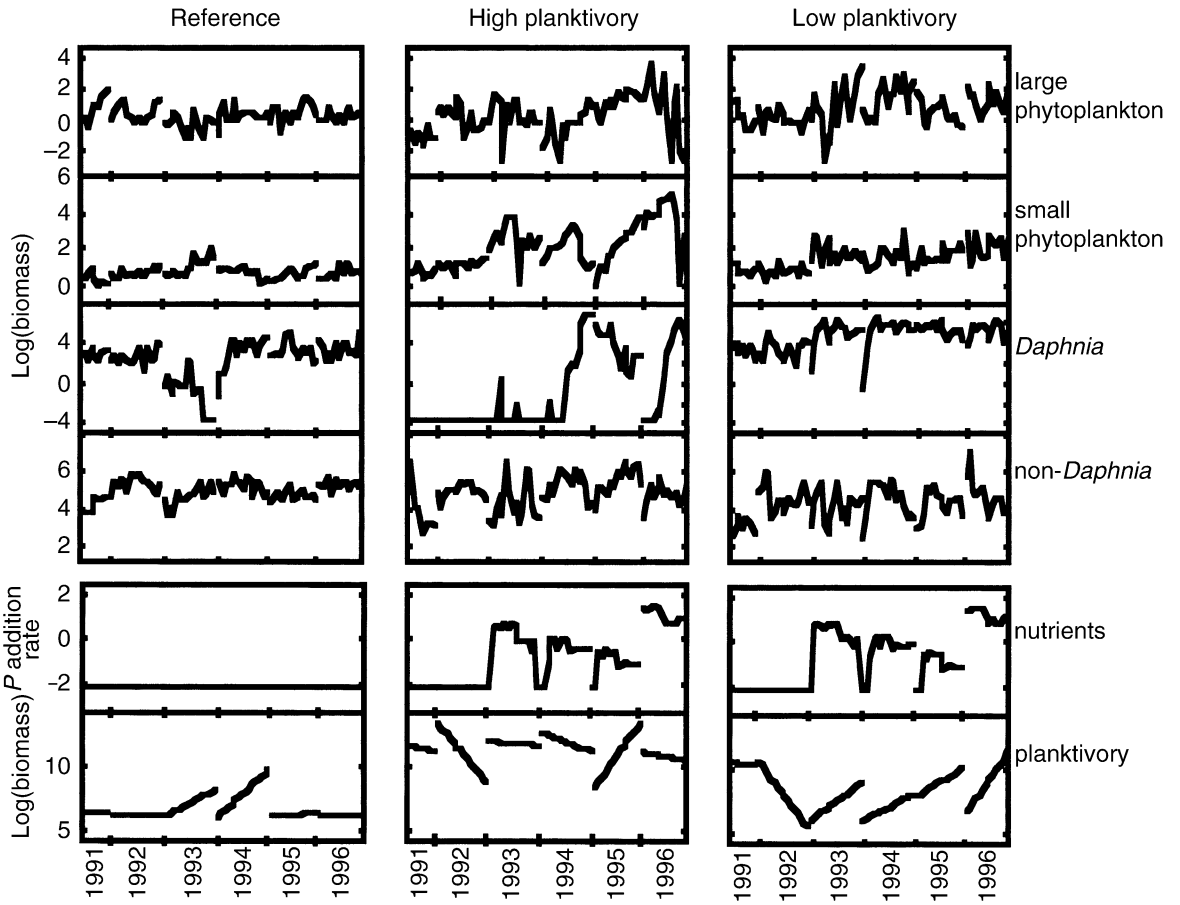

FIG. 5. Data from the limnological example. The top four panels for each lake give the log biomasses of the variates: large phytoplankton, small phytoplankton, *Daphnia*, and non-*Daphnia*. The total number of sample points for each lake is 91. Data are plotted as consecutive samples, with the lines broken between years. The lower two panels for each lake give the rate of nutrient (phosphorus) addition in the experimentally manipulated lakes and the log-biomass of planktivorous fish. The planktivorous fish biomasses were estimated only at the beginning and end of the summer stratification, so we interpolated the data for the analyses.

estimates of the variances of observation errors in variates and covariates, σ_g^2 and σ_h^2, respectively. For the two phytoplankton and two zooplankton variates, we set σ_g^2 to 0.04 and 0.16, respectively. These correspond to standard deviations of 0.2 and 0.4, which are roughly twice the standard deviations estimated by Carpenter et al. (1994*a*) for phytoplankton and zooplankton; for the present analysis we doubled the previous estimates to magnify the potential effects of observation error. Thus, on a log scale the observed values of the phytoplankton and zooplankton densities have a roughly 95% chance of lying within ± 0.4 and ± 0.8 units. The planktivory covariate was given an observation variance of 0.36, corresponding to a standard deviation of 0.6; this corresponds roughly to the typical observation error for planktivorous fish obtained using sampling methods similar to those used for our data (He 1990). Incorporating observation error in a covariate requires specifying its autocorrelation structure and treating it as a variate of a state-space model (e.g., Eq. 35). Because planktivory was interpolated from two points each summer, it cannot easily be incorporated into a state–space model. Nonetheless, we treated interpolated planktivory data as an AR(1) process. The first-order autocorrelation of planktivory, estimated simultaneously with the other model parameters, was high (0.97); although this is an artifact of the interpolation, the true autocorrelation in planktivory will also be high, since abundances of planktivorous fish will change slowly over a summer relative to changes in zooplankton and phytoplankton abundances. Because nutrient loading was experimentally manipulated, we assumed it had no observation error.

For fitting the observation–error model (Eq. 28), we factored out changes in variates between the end of summer in one year and the beginning of summer in the next year by restarting the Kalman filter procedure each year. The initial values of the variates each year were set equal to the observed values in the initial samples, and the initial estimates of the variance of the

TABLE 1. Parameter estimates and bootstrapped 95% confidence intervals for the AIC best-fitting autoregressive model, Eq. 27, fit to the limnological data using CLS estimation.

A) Fit of the model

Variate	Total R^2	Conditional R^2
Large phytoplankton	0.31	0.27
Small phytoplankton	0.74	0.34
Daphnia	0.91	0.17
Non-*Daphnia*	0.44	0.25

B) Parameter estimates for interactions between variates

Parameter	Large phytoplankton	Small phytoplankton	*Daphnia*	Non-*Daphnia*
$\mathbf{B_R}$ (reference lake)				
Large phytoplankton	0.50 [0.36, 0.58]			
Small phytoplankton		0.61 [0.47, 0.68]	−0.019 [−0.032, −0.004]	
Daphnia			0.76 [0.64, 0.82]	0
Non-*Daphnia*		0.10 [0.014, 0.20]	0	0.56 [0.43, 0.63]
$\mathbf{B_H}$ (high planktivory lake)				
Large phytoplankton	0.50 [0.36, 0.58]			
Small phytoplankton	−0.077 [−0.19, 0.04]	0.61 [0.47, 0.68]	−0.019 [−0.032, −0.004]	
Daphnia		0.33 [0.15, 0.56]	0.95 [0.91, 0.97]	0
Non-*Daphnia*		0.10 [0.014, 0.20]	0	0.56 [0.43, 0.63]
$\mathbf{B_L}$ (low planktivory lake)				
Large phytoplankton	0.50 [0.36, 0.58]	−0.36 [−0.68, −0.05]		
Small phytoplankton		0.072 [−0.13, 0.21]	−0.019 [−0.032, −0.004]	−0.10 [−0.27, −0.04]
Daphnia			0.76 [0.64, 0.82]	0
Non-*Daphnia*		0.10 [0.01, 0.20]	0	0.56 [0.43, 0.63]

C) Parameter estimates for the effects of covariates on variates, **C**

Parameter	Nutrient addition	Planktivory
Large phytoplankton	0.19 [0.08, 0.33]	0
Small phytoplankton	0.31 [0.25, 0.40]	0
Daphnia	0	−0.14 [−0.26, −0.03]
Non-*Daphnia*	0	−0.047 [−0.12, 0.02]

Note: Units are: zooplankton, log(mg dry mass/m^2); phytoplankton, log(mg chlorophyll/m^2), nutrient addition, mg $P \cdot m^{-2} \cdot d^{-1}$; planktivory, log($g$).

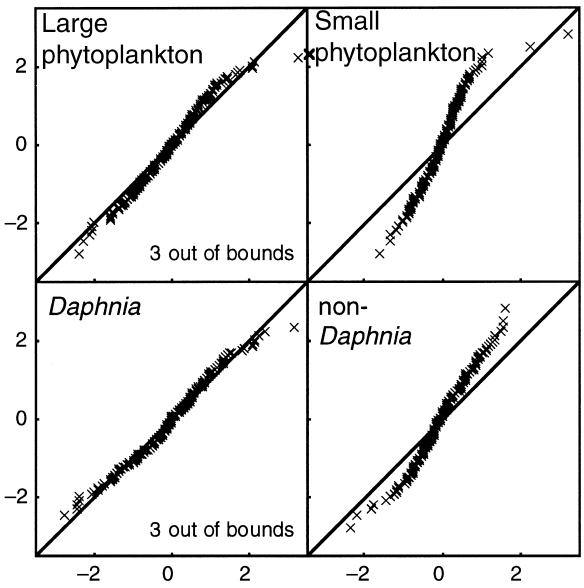

FIG. 6. Normal probability plots of the residuals for the four variates from the AIC best-fitting model using CLS parameter estimates.

process error each year were set to the global estimated value (Harvey 1989).

The coefficient estimates in the observation-error model are similar to the CLS estimates. The largest differences occurred for the intraspecific effect of small phytoplankton on itself in the low planktivory lake (0.072 for CLS; 0.25 with observation error) and for the effect of *Daphnia* on small phytoplankton (−0.02 for CLS; −0.17 with observation error). Other parameter estimates increased or decreased, demonstrating that observation error can have different effects on different coefficients in the MAR(1) model.

The parameter estimates from the MAR(1) models make ecological sense. *Daphnia* had a negative effect on small phytoplankton, as expected from this effective grazer (Vanni 1986, Carpenter and Kitchell 1993). The non-*Daphnia* zooplankton had a measurable negative effect on small phytoplankton only in the low planktivory lake. Small phytoplankton had a positive effect on the non-*Daphnia* group in all lakes, and had a strong positive effect on *Daphnia* in the high planktivory lake, which experienced a strong response of small phytoplankton to nutrient addition. The lack of a detectable effect of small phytoplankton on *Daphnia* in the ref-

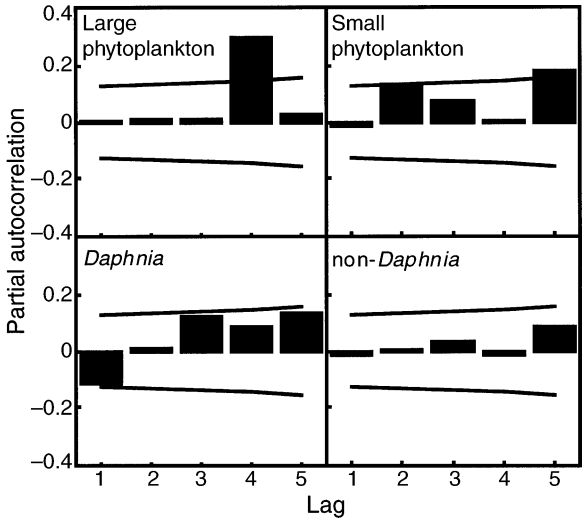

FIG. 7. Partial autocorrelation coefficients of residuals (PACFs) for the four variates in the AIC best-fitting autoregressive model with CLS parameter estimates (Table 1). Lines give the approximate 95% confidence limits calculated as ± 2 SE, where SE $= T^{-1/2}$ and T is the length of the set of residuals (Box et al. 1994:68). The length of the set of residuals changed from 237 (lag 1) to 165 (lag 5), because partial autocorrelation between points from different years were not included.

erence and low planktivory lakes is likely due to the low variance of small phytoplankton in these lakes. Detectable competitive interactions between large and small phytoplankton only occurred in the high and low planktivory lakes. Nutrient input had greater impact on small phytoplankton than large phytoplankton. Surface area/volume considerations suggest that small phytoplankton exploit nutrients more effectively than large phytoplankton (Chisholm 1992). Planktivory had greater impact on *Daphnia* than on non-*Daphnia*. This is consistent with the preference for *Daphnia* shown by size-selective planktivores (Brooks and Dodson 1965, Hall et al. 1976).

Comparison of stability among lakes

We used several measures to quantify the stability of the three lakes (Table 3). To measure stability in terms of the variance of the stationary distribution relative to the variance of the process (environmental) error, we computed the eigenvalues of **B** (Eqs. 22 and 23) and $\det(\mathbf{B})^{2/p}$ (Eq. 24) from the CLS parameter estimates for each lake. The return rate of the transition distribution to the stationary distribution is measured by the dominant eigenvalue of **B**, $\max(\lambda_{\mathbf{B}})$, which gives the asymptotic rate of return of the mean (Eq. 19), and the dominant eigenvalue of $\mathbf{B} \otimes \mathbf{B}$, $\max(\lambda_{\mathbf{B}\otimes\mathbf{B}})$, which gives the asymptotic rate of return of the variance (Eq. 21). Finally, to measure reactivity, we used both

TABLE 2. Parameter estimates for the AIC best-fitting model fit to the limnological data using ML estimation, Eqs. 27 and 38, and the observation-error model, Eq. 28.

A) Parameter estimates for interactions between variates

	ML				Observation error			
Variate	Large phyto-plankton	Small phyto-plankton	*Daphnia*	Non-*Daphnia*	Large phyto-plankton	Small phyto-plankton	*Daphnia*	Non-*Daphnia*
$\mathbf{B}_\mathbf{R}$ (reference lake)								
Large phytoplankton	0.50				0.48			
Small phytoplankton		0.60	−0.02			0.70	−0.17	
Daphnia			0.77	0			0.74	0
Non-*Daphnia*		0.10	0	0.55		0.10	0	0.60
$\mathbf{B}_\mathbf{H}$ (high plankitovory lake)								
Large phytoplankton	0.50				0.48			
Small phytoplankton	−0.066	0.60	−0.02		−0.076	0.68	−0.17	
Daphnia		0.34	0.95	0		0.36	0.97	0
Non-*Daphnia*		0.10	0	0.55		0.10	0	0.60
$\mathbf{B}_\mathbf{L}$ (low planktivory lake)								
Large phytoplankton	0.50	−0.39			0.48	−0.39		
Small phytoplankton		0.076	−0.02	−0.10		0.25	−0.17	−0.11
Daphnia			0.77	0			0.74	0
Non-*Daphnia*		0.10	0	0.55		0.10	0	0.60

B) Parameter estimates for the effects of covariates on variates **C**

	ML		Observation error	
Variate	Nutrient addition	Planktivory	Nutrient addition	Planktivory
Large phytoplankton	0.20	0	0.25	0
Small phytoplankton	0.32	0	0.25	0
Daphnia	0	−0.13	0	−0.14
Non-*Daphnia*	0	−0.048	0	−0.045

TABLE 3. Stability measures for the AIC best-fitting autoregressive model, Eq. 10, with parameters estimated using CLS.

Parameter	Reference	High planktivory	Low planktivory
Eigenvalues	0.74 [0.64, 0.82]	0.93 [0.88, 0.96]	0.74 [0.64, 0.82]
	0.59 [0.47, 0.68]	0.60 [0.49, 0.71]	0.51 [0.37, 0.62]
	0.54 [0.43, 0.63]	0.54 [0.43, 0.63]	0.48† [0.36, 0.58]
	0.48 [0.36, 0.58]	0.48 [0.36, 0.58]	0.07† [−0.12, 0.25]
$\det(\mathbf{B})^{2/p}$	0.33 [0.27, 0.39]	0.38 [0.31, 0.44]	0.12 [0.03, 0.22]
$\max(\lambda_{\mathbf{B}\otimes\mathbf{B}})$	0.55 [0.42, 0.67]	0.86 [0.78, 0.93]	0.55 [0.41, 0.67]
$-\mathrm{tr}(\boldsymbol{\Sigma})/\mathrm{tr}(\mathbf{V}_\infty)$	−0.58 [−0.67, −0.47]	−0.24 [−0.32, −0.14]	−0.60 [−0.70, −0.49]
$\max(\lambda_{\mathbf{B}'\mathbf{B}}) - 1$	−0.45 [−0.58, −0.25]	0.07 [−0.08, 0.30]	−0.44 [−0.57, −0.25]

† In 43 of 2000 bootstrapped data sets, two eigenvalues for the low planktivory lake were complex. These are ignored in calculating the 95% confidence bounds (shown in brackets).

$-\mathrm{tr}[\boldsymbol{\Sigma}]/\mathrm{tr}[\mathbf{V}_\infty]$ (Eq. 25) and $\max(\lambda_{\mathbf{B}'\mathbf{B}}) - 1$ (Eq. 26). To calculate $-\mathrm{tr}[\boldsymbol{\Sigma}]/\mathrm{tr}[\mathbf{V}_\infty]$, it is necessary to compute the covariance matrices for the process error and stationary distribution for each lake. For the covariance matrix of process errors, $\boldsymbol{\Sigma}$, we used the residuals from the data for each lake when all three lakes were fitted simultaneously. We then calculated the stationary distribution from Eq. 17 using the lake-specific matrices $\mathbf{B}$. All of these measures of stability factor out the variability caused by covariates and therefore assess the dynamics around the conditional stationary distribution for fixed values of the covariates.

Comparison of the eigenvalues of $\mathbf{B}$ for the three lakes reveals two patterns. First, the maximum eigenvalue in the high planktivory lake is much larger than the other two lakes. This is due to the large coefficient of *Daphnia* on itself, b_{33}, in $\mathbf{B}_\mathbf{H}$ (Table 1), indicating that the dynamics of *Daphnia* in the high planktivory lake are highly autocorrelated and show near-random-walk behavior. Second, the minimum eigenvalue for the low planktivory lake is much smaller than the other two lakes. This is due to the small value of the coefficient of small phytoplankton on itself, b_{22}, in $\mathbf{B}_\mathbf{L}$ (Table 1), indicating that the dynamics of small phytoplankton are highly intraspecifically regulated. These two patterns explain differences among the results of the remaining measures of stability.

When measured by $\det(\mathbf{B})^{2/p}$, the low planktivory lake is the most stable of the lakes; the lack of overlap of the 95% confidence intervals of $\det(\mathbf{B})^{2/p}$ for the low planktivory lake and the other two lakes provides strong statistical support for this difference. In contrast, the other measures of stability identify the high planktivory lake as the least stable, but do not distinguish between the reference and low planktivory lakes. The high planktivory lake has slower rates of returns of the mean and variance of the transition distribution to the stationary distribution ($\max(\lambda_\mathbf{B})$ and $\max(\lambda_{\mathbf{B}\otimes\mathbf{B}})$) and has greater reactivity ($\max(\lambda_{\mathbf{B}'\mathbf{B}}) - 1$ and $-\mathrm{tr}[\boldsymbol{\Sigma}]/\mathrm{tr}[\mathbf{V}_\infty]$). This contrast between $\det(\mathbf{B})^{2/p}$ and the other measures of stability can be explained by differences in the eigenvalues of the $\mathbf{B}$ matrices. The dominant eigenvalue corresponds to the ''slowest'' dimension of the multidimensional dynamics; specifically, the approach of the transition distribution to the stationary distribution is slowest in the direction given by the eigenvector corresponding to the dominant eigenvalue. Because the dominant eigenvalue for the high planktivory lake is greater than the other two lakes, measures of stability that are influenced strongly by the dominant eigenvalue of $\mathbf{B}$ distinguish this lake from the other two. Not only are the rates of return of the mean and variance of the transition distribution to the stationary distribution dictated by the dominant eigenvalue, reactivity is also strongly influenced by the ''slowest'' dimension of the system. In contrast, $\det(\mathbf{B})^{2/p}$ measures the size of the stationary distribution relative to the size of the distribution of process error. Because $\det(\mathbf{B})^{2/p}$ depends on all of the eigenvalues and hence all of the dimensions of the system, it is sensitive to the low value of the smallest eigenvalue found for the low planktivory lake.

TABLE 4. Stability measured by $\max(\lambda_\mathbf{B})$ and $\det(\mathbf{B})^{2/P}$ for the AIC best-fitting model with parameters estimated with CLS (Eq. 10), ML (Eq. 38), and observation error (Eq. 28).

Parameter and estimation method	Reference	High planktivory	Low planktivory
$\max(\lambda_\mathbf{B})$			
CLS	0.74	0.93	0.74
ML	0.76	0.93	0.76
Observation error	0.74	0.95	0.74
$\det(\mathbf{B})^{2/p}$			
CLS	0.33	0.38	0.12
ML	0.36	0.40	0.14
Observation error	0.38	0.44	0.24

To compare estimates of stability obtained from parameter estimates by CLS, ML, and our observation–error model, Table 4 gives estimates of $\max(\lambda_\mathbf{B})$ and $\det(\mathbf{B})^{2/p}$ for all three parameter estimation procedures. All three sets of estimates are similar, with the greatest difference being the increase in $\det(\mathbf{B})^{2/p}$ for the low planktivory lake with the inclusion of observation error, reflecting the increase in the smallest eigenvalue with observation error (Table 2).

Finally, we determined the sensitivity of the stability estimates to observation error by varying the magnitude of the predetermined observation error relative to the process error and calculating stability according to

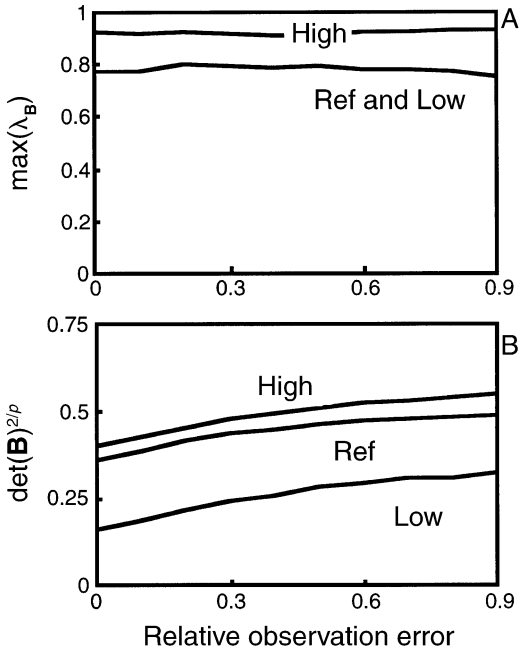

FIG. 8. The sensitivity of two measures of stability of the reference, high planktivory, and low planktivory lakes to observation error. (A) gives the dominant eigenvalue of **B**, $\max(\lambda_{\mathbf{B}})$, and (B) gives $\det(\mathbf{B})^{2/p}$. For the variates and covariate (planktivory), the "relative observation error" is the ratio of the observation error variance to the variance of the unobserved process error, g (Eq. 28).

$\max(\lambda_{\mathbf{B}})$ (Eq. 22) and $\det(\mathbf{B})^{2/p}$ (Eq. 24). We set the variance of observation errors $\mathbf{G}_t$ and $\mathbf{H}_t$ (Eq. 28) equal to g times the variances of the process errors $\mathbf{E}_t$ and ξ_t. Thus, g is related to reliability ratio K (Fuller 1987:5) by $g = (1 - K)/K$. As g increases from zero, relatively more of the total error in the observed variates and covariates is attributed to observation error. We restricted the analysis to the model structure of the best-fitting AIC model (Table 1).

Increasing observation error has little effect on $\max(\lambda_{\mathbf{B}})$ (Fig. 8A). With increasing values of observation error variance, the values of $\det(\mathbf{B})^{2/p}$ increase for all lakes (Fig. 8B), thus implying that accounting for observation error leads to decreases in the estimates of stability of the systems. Note, however, that values of $\det(\mathbf{B})^{2/p}$ in all lakes increase in parallel, so observation error has not affected our conclusions about the relative stabilities of the three lakes as measured by $\det(\mathbf{B})^{2/p}$.

Why are the stability properties of the lakes different?

By all measures of stability, the low planktivory lake is more stable than the high planktivory lake, whereas the reference lake has similar stability to the high planktivory lake when measured by $\det(\mathbf{B})^{2/p}$ but similar stability to the low planktivory lake when measured by the other stability properties. Since the reference lake was unmanipulated, our measures of stability did not simply identify the lakes that experienced the greatest experimental disturbance. Furthermore, the standard deviations of log biomasses of small and large phytoplankton, *Daphnia*, and non-*Daphnia* were 0.66, 0.36, 2.0, and 0.52 in the reference lake; 1.1, 0.66, 1.3, and 0.88 in the low planktivory lake; and 1.3, 1.2, 3.8, and 0.92 in the high planktivory lake. With the exception of *Daphnia*, the variability of plankton in the reference lake was lower than the other two lakes, and *Daphnia* variability was only moderately higher than in the low planktivory lake (2.0 vs. 1.3). Therefore, our measures of stability did not simply identify the lakes with higher variability. This is because all of the measures of stability are determined by the endogenous processes summarized by the **B** matrix in the MAR(1) model. The measures of stability assess how systems respond to environmental fluctuations, not how variable the systems are; more stable systems are those that respond less to the same severity of environmental fluctuations.

Visualizing the differences in stability among lakes is complicated by the two sources of environmental variability that differed among lakes: variability in the covariates $\mathbf{U}_t$ and process error $\mathbf{E}_t$. To portray the data in a way that equalizes both types of environmental variability, we generated time series from the equation

$$\mathbf{x}_t = \hat{\mathbf{B}}\mathbf{x}_{t-1} + \mathbf{e}_t \tag{39}$$

where $\hat{\mathbf{B}}$ is the estimated **B** matrix (different for different lakes), and $\mathbf{e}_t$ are CLS residuals for each lake divided by their within-lake standard deviation; this division causes the variance of the process error to be the same for each lake. For the initial point of each year, we used the difference between the observed initial point and the mean of the stationary distribution that would occur if the covariates maintained their yearly mean values for each year. In order to give a univariate portrayal of the data, we then projected the time series $\mathbf{x}_t$ onto the axis given by the eigenvector corresponding to the dominant eigenvalue, $\max(\lambda_{\mathbf{B}})$, of the $\hat{\mathbf{B}}$ matrix for each lake. Along this axis, the time series are described by a univariate AR(1) process with the autoregression coefficient given by $\max(\lambda_{\mathbf{B}})$. The resulting plots in Fig. 9 are comparable to those of simulated AR(1) processes in Fig. 1.

Fig. 9 shows that abundances in the high planktivory lake wander slowly up and down, while abundances in the other two lakes are drawn more tightly to the mean of the stationary distribution (from Eq. 39, this mean is zero). For all three lakes, the eigenvector corresponding to $\max(\lambda_{\mathbf{B}})$ is nearly parallel to the axis of log *Daphnia* biomass; this is the reason the dominant eigenvalues for all three lakes are close to the coefficient for *Daphnia* on itself given by b_{33} in the **B** matrices. Thus, *Daphnia* is largely responsible for differences in stability among lakes as measured by $\max(\lambda_{\mathbf{B}})$, a result similar to that obtained by Cottingham and Schindler (2000) using deterministic measures of stability. The importance of *Daphnia* is also seen in the

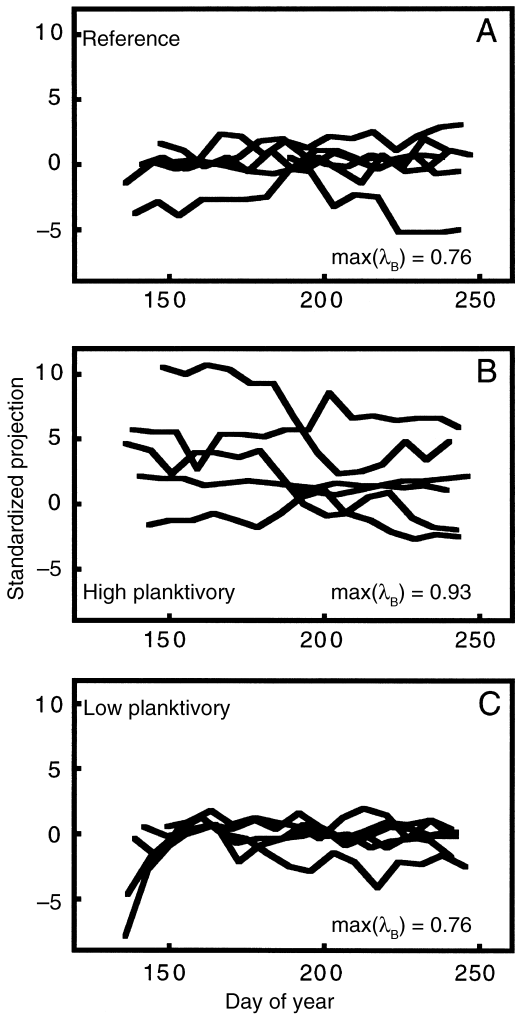

FIG. 9. Univariate depictions of the dynamics of the reference, high planktivory, and low planktivory lakes. The six lines in each panel give the dynamics in each of six years (Eq. 39). The vertical axis gives the projection of the log biomasses onto the eigenvector corresponding to the dominant eigenvalues of the estimates of **B** for each lake. The projections are standardized such that variances of the residuals along the eigenvectors are the same for each lake. Differences in dynamics caused by differences in the variances of the covariates in each lake are removed as described in the text (Eq. 39).

raw data in Fig. 5; despite experiencing quantitatively similar perturbations due to nutrient addition as the high planktivory lake, the abundances of *Daphnia* remained relatively constant in the low planktivory lake.

Biologically, the lack of self-regulation of *Daphnia* in the high planktivory lake was probably caused by high planktivory lowering *Daphnia* densities relative to the other lakes. With low *Daphnia* densities and corresponding high densities of small phytoplankton, the *Daphnia* population had the potential to increase, causing *Daphnia* densities to fluctuate more broadly in response to environmental variability.

A further difference in stability among lakes revealed by $\det(\mathbf{B})^{2/p}$ is the greater stability of the low planktivory lake caused by strong self-regulation of small phytoplankton (b_{22} in $\mathbf{B}_L$). This occurred even though the mean biomass of small phytoplankton was lower in the low planktivory than in the high planktivory lake during the experimental manipulations. The stability of the low planktivory lake could be a consequence of the high *Daphnia* abundance. Because *Daphnia* have a high phosphorus requirement, phosphorus recycling in lakes dominated by *Daphnia* may be slow, leading to nutrient limitation in the small phytoplankton (Elser et al. 1996). Nutrient limitation may contribute to the self-limitation term for small phytoplankton, b_{22}, estimated by the model.

Summary of limnological example

We fit a MAR(1) model to data from three lakes that were manipulated as part of an experiment to determine the response of phytoplankton and zooplankton to nutrient addition and planktivory. The MAR(1) identified interactions that were anticipated to be important on biological grounds. According to all of the measures of stability we used, the low planktivory lake was more stable than the high planktivory lake, whereas the reference lake was indistinguishable from either the low or high planktivory lakes depending on the measure of stability used. Analyses incorporating observation error did not change the general conclusions. The differences in stability among lakes were largely determined by the self-regulation of *Daphnia* and small phytoplankton, given by the corresponding diagonal terms of the **B** matrices.

DISCUSSION

MAR(1) models

We used MAR(1) models to characterize the stationary distribution and stability properties of multispecies time-series data. Is a MAR(1) process a biologically plausible model of an ecological community? Probably not, at least not in detail. But the more important question is: Can a MAR(1) model describe ecological interactions within communities and the stochastic characteristics of the dynamics they produce? For many communities, we believe the answer will be yes.

Many models of multispecies interactions are designed to explore different mechanisms that underlie population dynamics. Since many of these mechanisms involve nonlinearities, they demand nonlinear models (May and Oster 1976, Hastings et al. 1993, Carpenter et al. 1994*a*, Costantino et al. 1997, Ives et al. 2000*a*). In contrast to nonlinear mechanistic models, MAR(1) models give simple log-linear depictions of species interactions. This is not to say that MAR(1) models are not mechanistic. They include interactions among species and interactions between species and environmental factors. But they summarize these interactions as

linear dependencies of log population growth rates on log densities of species and (possibly transformed) environmental covariates. Thus, while MAR(1) can be viewed as purely empirical descriptions of data, they can also be used to explore the mechanisms by which species interactions affect multispecies dynamics.

An important advantage of using MAR(1) models is that their dynamical properties can be computed in a straightforward way. If a MAR(1) model is used as an approximation of a nonlinear process, then the stationary distribution computed from the MAR(1) model is likewise an approximation of the stationary distribution of the true nonlinear process. Interpreting a MAR(1) model as a log-linear approximation to a nonlinear process is appropriate when analyzing complex multispecies time series with multiple environmental covariates. Even though the underlying biological processes may be nonlinear, identifying these nonlinearities will be difficult unless they are very strong (Ives et al. 1999*a*). As a log-linear approximation, parameters in the MAR(1) model give the average strengths of species–species and species–environment interactions. When making comparisons among similar types of communities, as in our example of planktonic lake communities, potential biases caused by the log-linearity of MAR(1) models will likely be similar among communities, thereby reducing the chances of nonlinearities confounding the comparison of stability among communities.

Measures of stability

The three types of measures of stability that we defined for stochastic systems are similar in spirit to stability concepts applied in deterministic settings. The most frequently used deterministic measure of stability is the characteristic return rate, as measured by the dominant eigenvalue of the community matrix (May 1974). The interaction matrix **B** in a MAR(1) model serves the same role as the community matrix, with the dominant eigenvalue of **B** determining the characteristic return rate of the mean of the transition distribution to the mean of the stationary distribution. The square of the dominant eigenvalue measures the characteristic return rate of the variance of the transition distribution, so the variance of the transition distribution converges more rapidly to that of the stationary distribution than does the mean.

The suite of eigenvalues of **B** also measures the degree to which the environmental process error along the corresponding eigenvectors is amplified by species interactions, with greater amplification occurring for eigenvalues with larger magnitude. This amplification can be understood by referring to the deterministic result that the return rates to equilibrium along the eigenvectors are set by the corresponding eigenvalues. If eigenvalues are large, deterministic return rates are slow, and in the stochastic system the perturbations caused by environmental variability are not brought quickly back to the mean of the stationary distribution. The same idea underlies the concept of reactivity, which is based on the expected change in the distance from the mean of the stationary distribution from one time point to the next. If, on average, the expected change does not bring the population much closer to the mean, then the system will be less stable. High reactivity (when deviations do not tend strongly towards the mean) coincides with slow average return rates and eigenvalues of **B** with large magnitudes.

An important feature to all three types of stability measurements is that they separate endogenous and exogenous components of system variability. The endogenous component of variability is captured in the **B** matrix of species interactions, while exogenous sources are given as either measured environmental factors (covariates) or unmeasured environmental fluctuations (process error). What constitutes endogenous vs. exogenous components of variability is explicitly defined by the structure of the MAR(1) model. For example, if we had decided to focus only on phytoplankton in our analyses, we could have treated grazing by zooplankton as an exogenous factor, rather than an endogenous factor. In this case, *Daphnia* and non-*Daphnia* biomasses would be used as covariates rather than variates. Treating zooplankton as exogenous covariates would not change the CLS estimates for the coefficients of interactions between phytoplankton, although ML estimates might change, and the best-fitting model (as determined by the AIC or some other criterion) might include different interactions from the best-fitting model obtained when treating zooplankton as endogenous variates.

The measures of stability are most useful to make comparisons among systems. In our example of planktonic communities, our analyses identified the low planktivory lake as having higher stability than the high planktivory lake, with the reference lake similar to one or the other lake depending on the measure of stability applied. The most important result of the analyses is that they pose the question: Why are the dynamics of the three lakes different? The analyses give some general insight into the answer to this question; they finger *Daphnia* and small phytoplankton as the key groups in explaining the differences in stability among lakes. Nonetheless, we view this as only the starting point to understanding the stability of these planktonic communities.

Other stability properties

We have used components of the stationary distribution of population abundances to obtain measures of system stability, but other concepts of stability can be derived from other system characteristics. A common question asked about ecosystems is how much a system will change in response to a long-term environmental trend, such as climate change or lake eutrophication (Schindler 1974, Schindler et al. 1985, Frost et al. 1995). This question can be placed in the MAR(1) framework: How will mean species abundances change when there is a change in the mean value of one or

more covariates (Ives et al. 1999*a*)? All of the measures of stability we have developed apply to the time-invariant stationary distribution; even though we have included covariates, we have used these to factor out the time-dependency on long-term environmental trends so we can obtain information about the corresponding time-invariant stationary distribution determined by the **B** matrix. Nonetheless, the problem of how the mean of the stationary distribution would change in response to a change in the mean of the distribution of a covariate is related to the measures of stability we have derived.

As a simple example, consider the univariate AR(1) process given by

$$X_t = a + bX_{t-1} + cU_t + E_t. \quad (40)$$

If the covariate U_t is a stationary stochastic process with long-term mean ϕ_∞, then the mean of the stationary distribution of X_t is

$$\mu_\infty = \frac{a + c\phi_\infty}{1 - b}. \quad (41)$$

If a change $\Delta\phi$ in ϕ_∞ occurs, the corresponding change in μ_∞ is

$$\Delta\mu = \frac{c\Delta\phi}{1 - b}. \quad (42)$$

Thus, smaller values of b imply smaller changes in the mean of the stationary distribution relative to the change in the mean of the covariate U_t. This result is similar to that for the variance of the stationary distribution; Eq. 5 shows that the variance in the stationary distribution relative to the environmental variance equals $1/(1 - b^2)$, which decreases with b as long as b is positive. In the multivariate case, the change in the mean of the stationary distribution relative to changes in the mean of covariates can be calculated from the **B** matrix (Ives 1995*b*). Therefore, all of the statistical techniques we have described can be employed to predict how ecosystems will change in response to long-term environmental trends.

Another type of question that can be asked is whether the composition of a community remains stable in the face of environmental fluctuations, or whether species will be lost. In our analyses, we have assumed that extinction does not occur. Our analyses might give some information about which species in a community are at risk of extinction if, for example, species having low mean and high variance in abundance are more likely to drop to extinction. Nonetheless, this question is not addressed directly. Extinction implies that the MAR(1) process is not stationary and therefore requires investigating the properties of nonstationary processes (e.g., Chesson and Case 1986, Chesson 1994).

Conclusions

The chief advantage of MAR(1) models is that they can easily link data and theory, thereby making many theoretical ideas statistically testable. Thus, they allow the exploration of many theoretical ideas with data. Although we have focused on stability, other properties of species interactions could be tested using a MAR(1) framework. For example, it would be possible to test which species in a community are most sensitive to a particular environmental factor, or which species have relatively large impacts on other species in the community. It is also possible to use MAR(1) models to predict the response of communities to novel environmental disturbances if the effects of these disturbances on the population growth rates of different species are known (Ives et al. 1999*a*). Finally, although we have applied MAR(1) to community variables (biomass of different functional groups), the same techniques can be applied to ecosystem variables, such as primary productivity and nutrient content in different pools in an ecosystem.

Given the growing concerns about the effects of environmental disturbances on communities over large spatial and temporal expanses, MAR(1) models can give us insights into changes that we have already observed, and changes that we should anticipate.

Acknowledgments

We thank T. M. Frost, K. Gross, A. M. Kilpatrick, J. L. Klug, and J. Ripa for numerous conversations and insights about stability. Comments by N. J. Gotelli, K. Gross, J. Klug, J. Ripa, N. S. Urquhart, and two anonymous reviewers greatly improved the manuscript. N. S. Urquhart suggested Eq. A9, and he kindly allowed us to include it in the Appendix. This work was started at the "Community Dynamics" working group at the National Center for Ecological Analysis and Synthesis, Santa Barbara, California, USA, and was supported by additional grants from the National Science Foundation to A. R. Ives, B. Dennis, and S. R. Carpenter. The whole-lake manipulation experiments were supported by the National Science Foundation and the A. W. Mellon Foundation.

Literature Cited

Abrams, P. 1987. Indirect interactions between species that share a predator: varieties of indirect effects. Pages 38–54 *in* W. C. Kerfoot and A. Sih, editors. Predation. University Press of New England, Hanover, New Hampshire, USA.

Box, G. E. P., G. M. Jenkins, and G. C. Reinsel. 1994. Time series analysis: forecasting and control. Prentice Hall, Englewood Cliffs, New Jersey, USA.

Brooks, J. L., and S. I. Dodson. 1965. Predation, body size, and the composition of plankton. Science **150**:28–35.

Carpenter, S. R., J. J. Cole, J. R. Hodgson, J. F. Kitchell, M. L. Pace, D. Bade, K. L. Cottingham, T. E. Essington, J. N. Houser, and D. E. Schindler. 2001. Experimental enrichment of lakes with contrasting food webs. Ecological Monographs **71**:163–186.

Carpenter, S. R., K. L. Cottingham, and C. A. Stow. 1994*a*. Fitting predator–prey models to time series with observation errors. Ecology **75**:1254–1264.

Carpenter, S. R., T. M. Frost, A. R. Ives, J. F. Kitchell, and T. M. Kratz. 1994b. Complexity, cascades, and compensation in ecosystems. Pages 197–207 *in* M. Yasuno and M. M. Watanabe, editors. Biodiversity: its complexity and role. Symposium volume, National Institute for Environmental Studies, Japan.

Carpenter, S. R., and J. F. Kitchell. 1993. The trophic cascade in lakes. Cambridge University Press, Cambridge, UK.

Chesson, P. L. 1994. Multispecies competition in variable environments. Theoretical Population Biology **45**:227–276.

Chesson, P. L., and T. J. Case. 1986. Overview: nonequilibrium community theories: chance, variability, history and coexistence. Pages 229–239 *in* J. Diamond and T. J. Case, editors. Community ecology. Harper and Row, New York, New York, USA.

Chisholm, S. W. 1992. Phytoplankton size. Pages 213–237 *in* P. G. Falkowski and A. D. Woodhead, editors. Primary productivity and biogeochemical cycles in the sea. Plenum, New York, New York, USA.

Costantino, R. F., R. A. Desharnais, J. M. Cushing, and B. Dennis. 1997. Chaotic dynamics in an insect population. Science **275**:389–391.

Cottingham, K. L., and D. E. Schindler. 2000. Effects of grazer community structure on phytoplankton response to nutrient pulses. Ecology **81**:183–200.

Cronin, J. 1980. Differential equations: introduction and qualitative theory. Pure and applied mathematics, Volume 54. Marcel Dekker, New York, New York, USA.

Dennis, B., R. A. Desharnais, J. M. Cushing, and R. F. Costantino. 1995. Nonlinear demographic dynamics: mathematical models, statistical methods, and biological experiments. Ecological Monographs **65**:261–281.

Dennis, B., R. A. Desharnais, J. M. Cushing, S. M. Henson, and R. F. Costantino. 2001. Estimating chaos and complex dynamics in an insect population. Ecological Monographs **71**:277–303.

Dennis, B., W. P. Kemp, and M. L. Taper. 1998. Joint density dependence. Ecology **79**:426–441.

Dennis, B., P. L. Munholland, and J. M. Scott. 1991. Estimation of growth and extinction parameters for endangered species. Ecological Monographs **61**:115–143.

Dennis, B., and B. Taper. 1994. Density dependence in time series observations of natural populations: estimation and testing. Ecological Monographs **64**:205–224.

Efron, B., and R. J. Tibshirani. 1993. An introduction to the bootstrap. Chapman and Hall, New York, New York, USA.

Ehrlich, P. R., and G. C. Daily. 1993. Population extinction and saving biodiversity. Ambio **22**:64–68.

Elser, J. J., D. R. Dobberfuhl, N. A. MacKay, and J. H. Schampel. 1996. Organism size, life history, and N:P stoichiometry. BioScience **46**:674–684.

Frank, D. L., and S. J. McNaughton. 1991. Stability increases with diversity in plant communities: empirical evidence from the 1988 Yellowstone drought. Oikos **62**:360–362.

Frost, T. M., S. R. Carpenter, A. R. Ives, and T. K. Kratz. 1995. Species compensation and complementarity in ecosystem function. Pages 224–239 *in* C. G. Jones and J. H. Lawton, editors. Linking species and ecosystems. Chapman and Hall, New York, New York, USA.

Fuller, W. A. 1987. Measurement error models. John Wiley and Sons, New York, New York, USA.

Fuller, W. A. 1996. Introduction to statistical time series. John Wiley and Sons, New York, New York, USA.

Hall, D. J., S. T. Threlkeld, C. W. Burns, and P. H. Crowley. 1976. The size–efficiency hypothesis and the size structure of zooplankton communities. Annual Review of Ecology and Systematics **7**:177–208.

Harvey, A. C. 1989. Forecasting, structural time series models and the Kalman filter. Cambridge University Press, Cambridge, UK.

Harvey, A. C. 1993. Time series models. Harvester Wheatsheaf, New York, New York, USA.

Hastings, A., C. L. Hom, S. Ellner, P. Turchin, and H. C. J. Godfray. 1993. Chaos in ecology: is Mother Nature a strange attractor? Annual Review of Ecology and Systematics **34**:1–33.

He, X. 1990. Effects of predation on fish community: a whole lake experiment. Dissertation. University of Wisconsin, Madison, Wisconsin, USA.

Hilborn, R., and M. Mangel. 1997. The ecological detective: confronting models with data. Princeton University Press, Princeton, New Jersey, USA.

Holt, R. D. 1977. Predation, apparent competition, and the structure of prey communities. Theoretical Population Biology **12**:197–229.

Hooper, D. U., and P. M. Vitousek. 1997. The effects of plant composition and diversity on ecosystem processes. Science **277**:1302–1305.

Ives, A. R. 1995*a*. Measuring resilience in stochastic systems. Ecological Monographs **65**:217–233.

Ives, A. R. 1995*b*. Predicting the response of populations to environmental change. Ecology **76**:926–941.

Ives, A. R., S. R. Carpenter, and B. Dennis. 1999*a*. Community interaction webs and the response of a zooplankton community to experimental manipulations of planktivory. Ecology **80**:1405–1421.

Ives, A. R., K. Gross, and V. A. A. Jansen. 2000*a*. Periodic mortality events in predator–prey systems. Ecology **81**: 3330–3340.

Ives, A. R., K. Gross, and J. L. Klug. 1999*b*. Stability and variability in competitive communities. Science **286**:542–544.

Ives, A. R., J. L. Klug, and K. Gross. 2000*b*. Stability and species richness in complex communities. Ecology Letters **3**:399–411.

Judge, G. G., W. E. Griffiths, R. C. Hill, H. Lutkepohl, and T.-C. Lee. 1985. The theory and practice of econometrics. John Wiley and Sons, New York, New York, USA.

Klug, J. L., J. M. Fischer, A. R. Ives, and B. Dennis. 2000. Compensatory dynamics in planktonic community responses to pH perturbations. Ecology **81**:387–398.

Knight, K. 2000. Mathematical statistics. Chapman and Hall/CRC, Boca Raton, Florida, USA.

Lawton, J. H., and V. K. Brown. 1993. Redundancy in ecosystems. Pages 255–270 *in* E. D. Schulze and H. A. Mooney, editors. Biodiversity and ecosystem function. Springer-Verlag, Berlin, Germany.

MathWorks, I. 1996. MATLAB. The MathWorks, Natick, Massachusetts, USA.

May, R. M. 1974. Stability and complexity in model ecosystems. Second edition. Princeton University Press, Princeton, New Jersey, USA.

May, R. M., and G. F. Oster. 1976. Bifurcations and dynamic complexity in simply ecological models. American Naturalist **110**:573–599.

McCann, K., A. Hastings, and G. R. Huxel. 1998. Weak trophic interactions and the balance of nature. Nature **395**: 794–798.

McNaughton, S. J. 1977. Diversity and stability of ecological communities: a comment on the role of empiricism in ecology. American Naturalist **111**:515–525.

McNaughton, S. J. 1985. Ecology of grazing ecosystems: the Serengeti. Ecological Monographs **55**:259–294.

Neter, J., W. Wasserman, and M. H. Kutner. 1989. Applied linear regression models. Richard D. Irwin, Homewood, Illinois, USA.

Neubert, M. G., and H. Caswell. 1997. Alternatives to resilience for measuring the responses of ecological systems to perturbations. Ecology **78**:653–665.

Pace, M. L., J. J. Cole, S. R. Carpenter, and J. F. Kitchell. 1999. Trophic cascades revealed in diverse ecosystems. Trends in Ecology and Evolution **14**:483–488.

Paine, R. T. 1980. Food webs: linkage, interaction strength and community infrastructure. Journal of Animal Ecology **49**:667–685.

Persson, L. 1999. Trophic cascades: abiding heterogeneity and the trophic level concept at the end of the road. Oikos **85**:385–397.

Pimm, S. L. 1982. Food webs. Chapman and Hall, London, UK.

Pimm, S. L. 1984. The complexity and stability of ecosystems. Nature **307**:321–326.
Polis, G. A. 1999. Why are parts of the world green? Multiple factors control productivity and the distribution of biomass. Oikos **86**:3–15.
Press, W. H., S. A. Teukolsky, W. J. Vetterling, and B. P. Flannery. 1992. Numerical recipes in FORTRAN: the art of scientific computing. Cambridge University Press, Cambridge, UK.
Reddingius, J. 1971. Gambling for existence: a discussion of some theoretical problems in animal population ecology. Acta Biotheoretica **20**(Supplement):1–208.
Reinsel, G. C. 1997. Elements of multivariate time series analysis. Springer-Verlag, New York, New York, USA.
Schindler, D. W. 1974. Eutrophication and recovery in experimental lakes: implications for lake management. Science **184**:897–899.
Schindler, D. W., K. H. Mills, D. F. Malley, D. L. Findlay, J. A. Shearer, I. J. Davies, M. A. Turner, G. A. Linsey, and D. R. Cruikshank. 1985. Long-term ecosystem stress: the effects of years of experimental acidification on a small lake. Science **228**:1395–1401.
Schläpfer, F., and B. Schmid. 1999. Ecosystem effects of biodiversity: a classification of hypotheses and exploration of empirical results. Ecological Applications **9**:893–912.
Schnute, J. T. 1994. A general framework for developing sequential fisheries models. Canadian Journal of Fishery and Aquatic Science **51**:1676–1688.
Schulze, E. D., and H. A. Mooney. 1993. Biodiversity and ecosystem function. Springer-Verlag, Berlin, Germany.
Searle, S. R. 1982. Matrix algebra useful for statistics. John Wiley and Sons, New York, New York, USA.
Seber, G. A. F. 1984. Multivariate observations. John Wiley and Sons, New York, New York, USA.
Shenk, T. M., G. C. White, and K. P. Burnham. 1998. Sampling variance effects on detecting density dependence from temporal trends in natural populations. Ecological Monographs **68**:445–463.
Steinman, A. D., P. J. Mulholland, A. V. Palumbo, and D. L. DeAngelis. 1992. Lotic ecosystem response to a chlorine disturbance. Ecological Applications **2**:341–355.
Tilman, D. 1996. Biodiversity: population versus ecosystem stability. Ecology **77**:350–363.
Tilman, D., and J. A. Downing. 1994. Biodiversity and stability in grassland. Nature **367**:363–365.
Tilman, D., J. Knops, D. Wedin, P. Reich, M. Ritchie, and E. Siemann. 1997. The influence of functional diversity and composition on ecosystem processes. Science **277**:1300–1302.
Tong, Y. L. 1990. The multivariate normal distribution. Springer-Verlag, New York, New York, USA.
Vanni, M. J. 1986. Competition in zooplankton communities: suppression of small species by *Daphnia pulex*. Limnology and Oceanography **31**:1039–1056.
Vitousek, P. M. 1990. Biological invasions and ecosystem processes: towards an integration of population biology and ecosystem studies. Oikos **57**:7–13.
Vitousek, P. M., and D. U. Hooper. 1993. Biological diversity and terrestrial ecosystem biogeochemistry. Pages 3–14 *in* E. D. Schulze and H. A. Mooney, editors. Biodiversity and ecosystem function. Springer-Verlag, Berlin, Germany.
Walker, B. H. 1992. Biodiversity and ecological redundancy. Conservation Biology **6**:18–23.
Zeng, Z., R. M. Nowierski, M. L. Taper, B. Dennis, and W. P. Kemp. 1998. Complex population dynamics in the real world: modeling the influence of time-varying parameters and time lags. Ecology **79**:2193–2209.

APPENDIX

Derivation of Stability Properties

Variance of the stationary distribution

The first of the two methods we use to measure the variance of the stationary distribution relative to the variance of the distribution of the process error (Eqs. 22 and 23) involves transforming matrix $\mathbf{B}$ according to axes given by its eigenvectors (Ives 1995*a*). Specifically, $\mathbf{B}$ can be written in real canonical form (Cronin 1980) as $\mathbf{B} = \mathbf{SJS}^{-1}$, where $\mathbf{J}$ is a block-diagonal matrix whose elements consist of either a real eigenvalue of $\mathbf{B}$ (the scalar λ), or a 2×2 matrix of the form $[[\alpha, \beta], [-\beta, \alpha]]$ corresponding to a pair of complex conjugate eigenvalues $\alpha \pm \beta i$ of $\mathbf{B}$. Matrix $\mathbf{S}$ consists of the eigenvectors associated with the eigenvalues of $\mathbf{J}$; the real eigenvectors corresponding to real eigenvalues are entered as columns of $\mathbf{S}$, while complex conjugate pairs of eigenvectors corresponding to complex pairs of eigenvalues are entered as two columns, one containing the real and the other the imaginary parts of the eigenvectors. Matrix $\mathbf{S}$ can be used to transform the autoregressive process (Eq. 10) into a new coordinate system given by the eigenvectors of $\mathbf{B}$. Let $\tilde{\mathbf{X}}_t = \mathbf{SX}_t$ and $\tilde{\mathbf{E}}_t = \mathbf{SE}_t$ be, respectively, vectors containing linear combinations of the population densities and process errors in the new coordinate system, and let $\tilde{\mathbf{A}} = \mathbf{SA}$. Then from Eq. 10

$$\tilde{\mathbf{X}}_t = \mathbf{SX}_t = \mathbf{SA} + \mathbf{SBX}_{t-1} + \mathbf{SE}_t = \tilde{\mathbf{A}} + \mathbf{J}\tilde{\mathbf{X}}_{t-1} + \tilde{\mathbf{E}}_t. \quad \text{(A.1)}$$

Thus, the transformation produces a description of the autoregressive process in which species interactions are encapsulated in the block-diagonal matrix $\mathbf{J}$. The covariance matrix of the environmental variables in the new coordinate system is $\mathbf{\Psi} = \mathbf{S\Sigma S}'$.

Since $\mathbf{J}$ is a block-diagonal matrix, along the eigenvectors corresponding to a real eigenvalue λ, the dynamics are given by an equation of the form

$$\tilde{X}_t = \tilde{a} + \lambda\tilde{X}_{t-1} + \tilde{E}_t \quad \text{(A.2)}$$

where $\tilde{X}_t$ and $\tilde{E}_t$ are the population densities and process errors along the same eigenvector. Thus, from Eq. 7 the variance in the stationary distribution along this eigenvector is

$$\tilde{v}_\infty = \psi^2/(1 - \lambda^2) \quad \text{(A.3)}$$

where ψ^2 is the corresponding diagonal element of the covariance matrix $\mathbf{\Psi}$. This is Eq. 22 in the text.

A similar result can be obtained for complex eigenvalues. In the plane defined by the columns of $\mathbf{S}$ consisting of real and imaginary components of a complex set of eigenvectors corresponding to an eigenvalue pair $\alpha \pm \beta i$, the dynamics are given by

$$\tilde{X}^r_t = \tilde{a} + \alpha\tilde{X}^r_{t-1} + \beta\tilde{X}^c_{t-1} + \tilde{E}^r_t$$
$$\tilde{X}^c_t = \tilde{a} - \beta\tilde{X}^r_{t-1} + \alpha\tilde{X}^c_{t-1} + \tilde{E}^c_t \quad \text{(A.4)}$$

where superscripts r and c denote values along the axes given by the real and imaginary components of the complex eigenvector pair, respectively. Ives (1995*a*) shows that the sum of variances along these axes is

$$\tilde{v}^r_\infty + \tilde{v}^c_\infty = (\psi^r + \psi^c)/(1 - \|\alpha \pm \beta i\|^2) \quad \text{(A.5)}$$

where $\|\alpha \pm \beta i\|$ is the magnitude of the eigenvalues $\alpha \pm \beta i$. This leads to Eq. 23 in the text.

Reactivity

Reactivity is a measure of how strongly short-term (over one time step) changes tend to bring population abundances towards the mean of the stationary distribution. Consider first the deterministic case. Let $\Delta\mathbf{x}_t = \mathbf{x}_t - \mathbf{x}_\infty$ be a vector of

departures of species abundances from their equilibrium values and consider the linear deterministic model

$$\Delta\mathbf{x}_t = \mathbf{B}\Delta\mathbf{x}_{t-1}. \tag{A.6}$$

For a given perturbation $\mathbf{x}_{t-1}$ from equilibrium, the squared Euclidean distance between $\mathbf{x}_{t-1}$ and $\mathbf{x}_\infty$ is $\|\Delta\mathbf{x}_{t-1}\|^2 = \Delta\mathbf{x}'_{t-1}\Delta\mathbf{x}_{t-1}$. How much farther from or nearer to equilibrium will $\mathbf{x}_t$ be? Scaling the difference between $\|\Delta\mathbf{x}_{t-1}\|^2$ and $\|\Delta\mathbf{x}_t\|^2$ by the initial magnitude of the perturbation, we find that

$$\frac{\|\Delta\mathbf{x}_t\|^2 - \|\Delta\mathbf{x}_{t-1}\|^2}{\|\Delta\mathbf{x}_{t-1}\|^2} = \frac{\Delta\mathbf{x}'_{t-1}\mathbf{B}'\mathbf{B}\Delta\mathbf{x}_{t-1}}{\Delta\mathbf{x}'_{t-1}\Delta\mathbf{x}_{t-1}} - 1. \tag{A.7}$$

The term $\Delta\mathbf{x}'_{t-1}\mathbf{B}'\mathbf{B}\Delta\mathbf{x}_{t-1}/\Delta\mathbf{x}'_{t-1}\Delta\mathbf{x}_{t-1}$ is known as the Raleigh quotient and can be used to calculate the ''worst-case'' scenario for the reactivity of the system (i.e., the maximum distance $\mathbf{x}_t$ will be from $\mathbf{x}_\infty$). If $\mathbf{B}$ has full rank (i.e., no eigenvalues are zero), then the symmetric matrix $\mathbf{B}'\mathbf{B}$ is positive definite (i.e., $\Delta\mathbf{x}'_{t-1}(\mathbf{B}'\mathbf{B})\Delta\mathbf{x}_{t-1} > 0$ for all nonzero vectors $\Delta\mathbf{x}_{t-1}$). Also, $\mathbf{B}'\mathbf{B}$ has all real and positive eigenvalues. The worst-case scenario is when the perturbation $\Delta\mathbf{x}_{t-1}$ happens to be in the same direction as the eigenvector of $\mathbf{B}'\mathbf{B}$ associated with the largest eigenvalue, $\max(\lambda_{\mathbf{B}'\mathbf{B}})$. In this case, the Raleigh quotient attains its maximum value of $\max(\lambda_{\mathbf{B}'\mathbf{B}})$, and the farthest distance from equilibrium that $\mathbf{x}_t$ can advance beyond $\mathbf{x}_{t-1}$ is $\max(\lambda_{\mathbf{B}'\mathbf{B}}) - 1$ (Eq. A.7 evaluated at its maximum value). Thus, $\max(\lambda_{\mathbf{B}'\mathbf{B}})$ is a measure of reactivity, with values of $\max(\lambda_{\mathbf{B}'\mathbf{B}}) > 1$ giving worst-case scenarios in which the system initially moves farther from equilibrium following a perturbation. On the other hand, when $\max(\lambda_{\mathbf{B}'\mathbf{B}}) < 1$ the system always moves immediately back towards equilibrium.

This analysis of the deterministic case is restricted to the worst-case scenario. For stochastic systems it is possible to ask how far, on average, is the system likely to change from one time step to the next with respect to the mean of the stationary distribution. Let $\mathbf{X}_t$ denote the random variable for the population size at time t, and let $\Delta\mathbf{X}_t = \mathbf{X}_t - \boldsymbol{\mu}_\infty$ be the difference between $\mathbf{X}_t$ and the mean of the stationary distribution. The expectation of $\Delta\mathbf{X}_t$ given $\Delta\mathbf{X}_{t-1}$ is $\mathrm{E}_{\varepsilon_{t-1}}[\Delta\mathbf{X}_t \,|\, \Delta\mathbf{X}_{t-1}] = \mathbf{B}\Delta\mathbf{X}_{t-1}$. Let $\|\mathrm{E}_{\varepsilon_{t-1}}[\Delta\mathbf{X}_t \,|\, \Delta\mathbf{X}_{t-1}]\|$ denote the squared Euclidean distance of the expectation of $\Delta\mathbf{X}_t$ given $\Delta\mathbf{X}_{t-1}$ from the mean of the stationary distribution, $\boldsymbol{\mu}_\infty$. Thus, if the Euclidean distance of a given value of $\Delta\mathbf{X}_{t-1}$ from $\boldsymbol{\mu}_\infty$ is $\|\Delta\mathbf{X}_{t-1}\|^2$, then the expectation for the change in distance from $\boldsymbol{\mu}_\infty$ between times $t-1$ and t is $\|\mathrm{E}_{\varepsilon_{t-1}}[\Delta\mathbf{X}_t \,|\, \Delta\mathbf{X}_{t-1}]\|^2 - \|\Delta\mathbf{X}_{t-1}\|^2$. Because $\Delta\mathbf{X}_{t-1}$ itself is a random variable, reactivity depends on the expectation taken over the distribution of $\Delta\mathbf{X}_{t-1}$, and to obtain a measure comparable to reactivity defined for deterministic systems (Eq. A.7), we define reactivity for stochastic systems as

$$\frac{\mathrm{E}_{\mathbf{X}_{t-1}}[\|\mathrm{E}_{\varepsilon_{t-1}}[\Delta\mathbf{X}_t \,|\, \Delta\mathbf{X}_{t-1}]\|^2] - \mathrm{E}_{\mathbf{X}_{t-1}}[\|\Delta\mathbf{X}_{t-1}\|^2]}{\mathrm{E}_{\mathbf{X}_{t-1}}[\|\Delta\mathbf{X}_{t-1}\|^2]}. \tag{A.8}$$

The smaller this quantity, the greater the tendency for the population to move towards the mean of the stationary distribution between successive time steps. Below we derive an expression for this quantity.

Because $\mathbf{B}'\mathbf{B}$ is a symmetric matrix, it can be decomposed such that $\mathbf{B}'\mathbf{B} = \mathbf{K}\boldsymbol{\vartheta}\mathbf{K}'$ where $\boldsymbol{\vartheta}$ is a diagonal matrix containing the eigenvalues of $\mathbf{B}'\mathbf{B}$, and $\mathbf{K}$ is a matrix with columns containing the corresponding eigenvectors. The matrix $\mathbf{B}'\mathbf{B}$ is positive definite and symmetric, and therefore its eigenvalues are real and its eigenvectors are orthogonal, so $\mathbf{K}\mathbf{K}' = \mathbf{I}$. Let $\mathbf{Z}_{t-1} = \mathbf{K}'\mathbf{X}_{t-1}$ be the population size measured with respect to axes given by the eigenvectors of $\mathbf{B}'\mathbf{B}$, and let $\boldsymbol{\nu}_{t-1} = \mathbf{K}'\boldsymbol{\mu}_{t-1}$ be the mean of $\mathbf{Z}_{t-1}$. Then

$$\begin{aligned}
&\mathrm{E}_{\mathbf{X}_{t-1}}[\|\mathrm{E}_{\varepsilon_{t-1}}[\Delta\mathbf{X}_t \,|\, \Delta\mathbf{X}_{t-1}]\|^2] \\
&\quad = \mathrm{E}_{\mathbf{X}_{t-1}}[\Delta\mathbf{X}'_{t-1}\mathbf{B}'\mathbf{B}\Delta\mathbf{X}_{t-1}] \\
&\quad = \mathrm{E}_{\mathbf{X}_{t-1}}[\{(\mathbf{X}_{t-1} - \boldsymbol{\mu}_{t-1}) + (\boldsymbol{\mu}_{t-1} - \boldsymbol{\mu}_\infty)\}' \\
&\qquad\qquad \times \mathbf{B}'\mathbf{B}\{(\mathbf{X}_{t-1} - \boldsymbol{\mu}_{t-1}) + (\boldsymbol{\mu}_{t-1} - \boldsymbol{\mu}_\infty)\}] \\
&\quad = \mathrm{E}_{\mathbf{X}_{t-1}}[(\mathbf{X}_{t-1} - \boldsymbol{\mu}_{t-1})'\mathbf{B}'\mathbf{B}(\mathbf{X}_{t-1} - \boldsymbol{\mu}_{t-1})] \\
&\qquad + (\boldsymbol{\mu}_{t-1} - \boldsymbol{\mu}_\infty)'\mathbf{B}'\mathbf{B}(\boldsymbol{\mu}_{t-1} - \boldsymbol{\mu}_\infty) \\
&\quad = \mathrm{E}_{\mathbf{Z}_{t-1}}[(\mathbf{Z}_{t-1} - \boldsymbol{\nu}_{t-1})\boldsymbol{\vartheta}(\mathbf{Z}_{t-1} - \boldsymbol{\nu}_{t-1})] \\
&\qquad + (\boldsymbol{\mu}_{t-1} - \boldsymbol{\mu}_\infty)'\mathbf{B}'\mathbf{B}(\boldsymbol{\mu}_{t-1} - \boldsymbol{\mu}_\infty) \\
&\quad = \sum_{i=1}^{p} \varphi_i\gamma_{ii} + (\boldsymbol{\mu}_{t-1} - \boldsymbol{\mu}_\infty)'\mathbf{B}'\mathbf{B}(\boldsymbol{\mu}_{t-1} - \boldsymbol{\mu}_\infty)
\end{aligned} \tag{A.9}$$

where φ_i are the eigenvalues of $\mathbf{B}'\mathbf{B}$ and γ_{ii} are the diagonal elements of the covariance matrix of $\mathbf{Z}_{t-1}$.

Eq. A.9 gives the general case for an arbitrary distribution of $\mathbf{X}_{t-1}$. To obtain the reactivity of the system averaged over a long time period, we can let the distribution of $\mathbf{X}_{t-1}$ be the stationary distribution, $\mathbf{X}_{t-1} = \mathbf{X}_\infty$. In this case, the second term in Eq. A.9 becomes zero, and γ_{ii} are the diagonal elements of the covariance matrix of stationary distribution transformed according to axes given by the eigenvectors of $\mathbf{B}'\mathbf{B}$. Thus, reactivity is given as

$$\frac{\mathrm{E}_{\mathbf{X}_\infty}[\|\mathrm{E}_{\varepsilon_{t-1}}[\Delta\mathbf{X}_t \,|\, \Delta\mathbf{X}_{t-1}]\|^2] - \mathrm{E}_{\mathbf{X}_\infty}[\|\Delta\mathbf{X}_{t-1}\|^2]}{\mathrm{E}_{\mathbf{X}_\infty}[\|\Delta\mathbf{X}_{t-1}\|^2]} = \frac{\sum_{i=1}^{p} \varphi_i\gamma_{ii}}{\sum_{i=1}^{p} \gamma_{ii}} - 1. \tag{A.10}$$

The reactivity of the process at the stationary distribution depends on the average of the eigenvalues of $\mathbf{B}'\mathbf{B}$ weighted by the variances of the stationary distribution γ_{ii}. The worst-case scenario is when all of the variance in the process error occurs along the eigenvectors corresponding to the dominant eigenvalue of $\mathbf{B}'\mathbf{B}$, $\max(\lambda_{\mathbf{B}'\mathbf{B}})$. In this case

$$\frac{\mathrm{E}_{\mathbf{X}_\infty}[\|\mathrm{E}_{\varepsilon_{t-1}}[\Delta\mathbf{X}_t \,|\, \Delta\mathbf{X}_{t-1}]\|^2] - \mathrm{E}_{\mathbf{X}_\infty}[\|\Delta\mathbf{X}_{t-1}\|^2]}{\mathrm{E}_{\mathbf{X}_\infty}[\|\Delta\mathbf{X}_{t-1}\|^2]} = \max(\lambda_{\mathbf{B}'\mathbf{B}}) - 1. \tag{A.11}$$

This leads to Eq. 26 in the text.

An alternative expression for reactivity in stochastic systems can be obtained for the case in which $\mathbf{X}_{t-1} = \mathbf{X}_\infty$. Because the expression $\Delta\mathbf{X}'_\infty\mathbf{B}'\mathbf{B}\Delta\mathbf{X}_\infty$ is in quadratic form, $\mathrm{E}_{\Delta\mathbf{X}_\infty}[\Delta\mathbf{X}'_\infty\mathbf{B}'\mathbf{B}\Delta\mathbf{X}_\infty] = \mathrm{tr}[\mathbf{B}'\mathbf{B}\mathbf{V}_\infty]$ (e.g., Judge et al. 1985: 16), the trace of the matrix product $\mathbf{B}'\mathbf{B}\mathbf{V}_\infty$. Furthermore, since $\mathbf{V}_\infty$ is symmetric, $\mathrm{tr}[\mathbf{B}'\mathbf{B}\mathbf{V}_\infty] = \mathrm{tr}[\mathbf{B}\mathbf{V}_\infty\mathbf{B}']$. Finally, from Eq. 16 $\mathrm{tr}[\mathbf{B}\mathbf{V}_\infty\mathbf{B}'] = \mathrm{tr}[\mathbf{V}_\infty] - \mathrm{tr}[\boldsymbol{\Sigma}]$. Thus, since $\mathrm{E}_{\mathbf{X}_\infty}[\|\mathrm{E}_{\varepsilon_{t-1}}[\Delta\mathbf{X}_t \,|\, \Delta\mathbf{X}_{t-1}]\|^2] = \mathrm{E}_{\mathbf{X}_\infty}[\Delta\mathbf{X}'_\infty\mathbf{B}'\mathbf{B}\Delta\mathbf{X}_\infty]$,

$$\frac{\mathrm{E}_{\mathbf{X}_\infty}[\|\mathrm{E}_{\varepsilon_{t-1}}[\Delta\mathbf{X}_t \,|\, \Delta\mathbf{X}_{t-1}]\|^2] - \mathrm{E}_{\mathbf{X}_\infty}[\|\Delta\mathbf{X}_{t-1}\|^2]}{\mathrm{E}_{\mathbf{X}_\infty}[\|\Delta\mathbf{X}_{t-1}\|^2]} = -\frac{\mathrm{tr}[\boldsymbol{\Sigma}]}{\mathrm{tr}[\mathbf{V}_\infty]}. \tag{A.12}$$

This is Eq. 25 in the text.

SUPPLEMENT

Programs and data for many of the analyses of the limnological data set are available in ESA's Electronic Data Archive: *Ecological Archives* M073-003-S1. Programs are written in Matlab (MathWorks 1996), and data are given as text files formatted to be accessed by the programs.